Modeling connectivity of walleye pollock in the Gulf of Alaska: Are there any linkages to the Bering Sea and Aleutian Islands?

by

Carolina Parada[a,b],Sarah Hinckley[c], John Horne[d], Michael Mazur[e], Albert Hermann[f], Enrique Curchister[g]

[a] To whom correspondence should be addressed. Departamento de Geofísica, Universidad de Concepción, Casilla 160-C, Concepción, Chile.
Phone: 56 (41) 2204136. FAX: 56-41-2220104. E-mail: carolina.parada@dgeo.udec.cl, carolina.parada.veliz@gmail.com
[b] Instituto Milenio de Oceanografía (IMO), Universidad de Concepción, Concepción, Chile
[c] Alaska Fisheries Science Center, NOAA, 7600 Sand Point Way NE, WA 98115, USA. E-mail: sarah.hinckley@noaa.gov
[d] University of Washington, School of Aquatic and Fishery Sciences, Box 355020, Seattle,WA 98195, USA. E-mail: jhorne@uw.edu
[e] U.S. Fish & Wildlife Service, 170 North First Street, Lander, Wyoming 82520. Email: michael_mazur@fws.gov
[f] Pacific Marine Environmental Laboratory, NOAA, 7600 Sand Point Way NE, WA 98115, USA. E-mail: Albert.J.Hermann@noaa.gov
[g] Institute of Marine and Coastal Sciences, Rutgers University, 71 Dudley Road, New Brunswick, NJ 08901-8521, USA. E-mail: enrique@marine.rutgers.edu

Running title: MODELLING CONNECTIVITY IN GULF OF ALASKA WALLEYE POLLOCK

Keywords: Modeling, transport process, larvae, juveniles, walleye pollock, connectivity, individual-based model, stock structure.

Abstract

We investigated the connectivity of walleye pollock in the Gulf of Alaska (GOA) and linkages to the Bering Sea (BS) and Aleutian Island (AL) regions. We used a spatially-explicit Individual-based model (IBM) coupled to 6 years of a hydrodynamic model that simulates the early life history of walleye pollock in the GOA (eggs to age-0 juveniles). The processes modeled included growth, movement, mortality, feeding and the bioenergetics component for larvae and juveniles. Simulations were set to release particles on the 1st of the month (February to May) in fourteen historical spawning areas in the GOA up to the 1st of September each year. Model results reproduced the link between the Shelikof Strait spawning area and the Shumagin nursery region for March and April spawners, besides other Potential Nursery Areas (PNAs) found in the GOA. A prominent finding of this study was the appearance of the BS as important PNAs for several GOA spawning grounds, which is supported by a consistent flow into the BS through Unimak Pass. The simulations showed the highest density of simulated surviving pollock in the western Bering Sea (WBS) region with the lowest coefficients of variation of the whole domain. Three spawning sectors were defined, which aggregate multiple spawning areas in the eastern (EGOA), central (CGOA) and western Gulf of Alaska (WGOA). A connectivity matrix showed strong retention within the CGOA (25.9%) and EGOA (23.8%), but not in the WGOA (7.2%). Within the GOA, the highest connectivity is observed from EGOA to CGOA (57.8%) followed by the connection from CGOA to WGOA (24.3%). Overall, one of the most prominent connections was from WGOA to WBS (62.8%), followed by a connection from CGOA to WBS (29.2%). In addition, scenarios of shifting spawning locations and nursery sectors of GOA, BS and AL are explored and implications for walleye pollock stock structure hypotheses are discussed.

1. Introduction

Walleye pollock (*Gadus chalcogrammus*) is a dominant component of the Gulf of Alaska (GOA) ecosystem, but knowledge of the biological and physical mechanisms that create variability in its recruitment is incomplete. Peak spawning at the major spawning areas in GOA occurs at different times. Adult walleye pollock are known to spawn from late March to early April at the southwestern end of Shelikof Strait, between Kodiak Island and mainland Alaska (Kendall *et al*., 1987; Schumacher and Kendall, 1991). Eggs are fertilized at depths between 150 and 200 m, and hatch after a period of about two weeks (Yoklavich and Bailey, 1990). These larvae rise to the upper 50 m of the water column and drift in prevailing currents for the next several weeks (late April through mid-May) (Yoklavich and Bailey, 1990). Larger larvae undergo diel migrations between 15 and 50 m (Kendall *et al*., 1994). Currents transport larvae southwest along the Alaska Peninsula (Fig.1), or offshore along the shoreward edge of the Shelikof sea valley southwest of Shelikof Strait (Yoklavich and Bailey, 1990; Hinckley *et al*., 2001). By mid-summer, many of the survivors (juvenile stage) have been advected to the Shumagin Islands, about 300 km southwest of the Shelikof spawning site (Hinckley *et al*., 1991). The prevailing hypothesis is that Shelikof Strait is the primary spawning area, and that the Shumagin Islands provide the main nursery area in the GOA (Hinckley *et al*., 2001). Another apparent spawning peak occurs between February 15 to March 1 in the Shumagin Islands area and surrounding areas, (Dorn *et al*., 2012). These secondary walleye pollock spawning areas have been observed in the GOA during acoustic surveys. The shelf break near Chirikof Island, the Shumagin area, Sanak Gully, Morzhovoi Bay and Marmot Bay (Fig. 1) satisfy the criterion of appearing in the acoustic surveys at least three times to be considered secondary spawning regions (Dorn *et al*., 2014). In addition, egg distribution data from ichthyoplankton surveys conducted by the Alaska Fisheries Science Center (AFSC, Ciannelli *et al*., 2007) have shown non-Shelikof spawning locations (Unimak Pass, Semidis and Shumagin Islands, Fig.1; Ciannelli *et al*., 2007). However, the role of these non-Shelikof spawning areas and their contribution to the GOA pollock stock remains uncertain.

GOA walleye pollock is currently managed as a single stock, independent of Bering Sea (BS) and Aleutian Islands (AL) walleye pollock. Within the GOA, there is evidence that distinguish (e.g. allozyme frequency and mtDNA) the Shelikof Strait spawning population from spawning populations in the northern GOA (Prince William Sound and Middleton Island), although some interannual genetic variability has been observed (Olsen *et al*., 2002). Despite this variability, evidence provided from the assessment of the stock structure following the template developed by the North Pacific Fishery Management Council) stock structure working group (Dorn *et al*., 2012) supports treating pollock in the eastern portion of the GOA separately from pollock in the central and western portions. Separation of walleye pollock in the GOA from those in the Eastern Bering Sea (EBS) is based on studies of larval drift from spawning locations (Bailey *et al*., 1997) and genetic studies based on allozyme frequencies (Grant and Utter 1980; Olsen *et al*. 2002), mtDNA variability (Mulligan *et al*., 1992; Shields and Gust 1995; Kim *et al*., 2000), and microsatellite allele variability (O'Reilly *et al*., 2004). Dorn *et al*. (2012) claim that results supporting the current separation of walleye pollock stocks in the GOA are equivocal, since the data used for the larval transport study (Bailey *et al*., 1997) did not encompass the entire range of the GOA, and genetic analyses have not provided definitive results on the separation or mixing of population components. However, examining how distributions of fish evolve between adult spawning locations and juvenile retention areas, may contribute to the understanding of early stage growth and survival, the connection between spawning and nursery areas, and population structure.

Population connectivity is inherently a coupled bio-physical research topic, involving physical processes such as jets, eddies, meanders, fronts, tides, island wakes and lateral intrusions (Cowen

and Spounagle, 2009). However, physical processes alone do not determine connectivity, because larval behavior such as vertical migration also plays a relevant role (Cowen *et al*., 2002). A connectivity matrix describes the spatial distribution of settlement destinations or nursery grounds of individuals that originate from a given source, as well as the links between both regions (Largier, 2003). The quantification of the probability of larvae reaching nursery areas, through transport, given specific spawning grounds determines the strength of the connectivity. Almost all fish have planktonic life stages that can spend days, weeks, or months drifting, eating, and growing in the pelagic zone (Gaines *et al*., 2007). Scales of dispersal can vary by more than six orders of magnitude, ranging from meters to hundreds of kilometers (Cowen *et al*., 2000; Gaines *et al*., 2007; Pineda *et al*., 2007). In regions with complex circulation patterns, trajectories of individual fish may differ widely, resulting in a wide range of exposures to environmental variables such as temperature, salinity, and to predator and prey interactions, resulting in variable growth and survival among individual larvae.

Connectivity can be estimated by tracking individuals (Largier, 2003). However, there are non-trivial logistic and operational constraints when tracking small aquatic organisms over hundreds of kilometers (Willis *et al*., 2003; Sale *et al*., 2005). Computer simulation models have therefore been used to increase the understanding of the kinematics of early life stages of several fish species, but the dispersal, survival, and connectivity between spawning and nursery areas remains unresolved for many marine populations (Beck *et al*., 2001; Cowen *et al*., 2007). Lagrangian-based, spatially-explicit Individual-Based Models (IBMs) can be used to track individuals from their release at spawning sites to nursery areas, and have been used in connectivity studies (e.g. Werner *et al*., 2001, North *et al*., 2009). Previous IBM models have explored the early life history of walleye pollock in the GOA (Hinckley *et al*., 1996; Hinckley *et al*., 2001; Megrey and Hinckley, 2001) by studying the impact of physical and biological factors on location timing of spawning for this species, and recruitment variability and the resulting spatial distributions.

In this study we used a spatially-explicit IBM – hydrodynamic coupled model to reveal early life stage (i.e. egg to age-0 juvenile) walleye pollock trajectories between spawning areas within the GOA and nursery areas in the GOA, BS, and AL region. The primary objective was to determine the relative importance of spawning times and locations to surviving age-0 walleye pollock juveniles in nursery areas during the fall of each year. In addition, scenarios of connectivity between spawning locations and recruitment of GOA, BS, and Al populations and implication for walleye pollock stock structure hypotheses are discussed.

2. Methods

The modeling approach consisted of the development of a biophysical model in which the Regional Ocean Modeling System (ROMS) is coupled with a modified version of the IBM for walleye pollock developed by Hinckley *et al* (1996) and Megrey and Hinckley (2001). The details of the biological model configuration and additions are briefly summarized in section 2.3.

We coupled ROMS outputs to a young walleye pollock IBM, modified from Hinckley *et al*. (2008). The hydrodynamic model produced daily averaged output consisting of salinity and temperature fields, and 3D velocities. These physical variables were used to drive the IBM model over the same years (1978, 1982, 1988, 1992, 1999, 2001) . The IBM operates on the same spatial grid as the hydrodynamic model (see below).

2.1 Hydrodynamic model configuration

The hydrodynamic model used in this work is the fourth generation of the Northeast Pacific model (NEP4) previously described by Curchitser *et al*. (2005), Hermann *et al*. (2009 a,b), and Cooper *et al*. (2013). This model has been used to examine the drift and transport of a variety of North Pacific marine species including Greenland halibut (Duffy-Anderson *et al.,* 2013). It is based on the ROMS (Shchepetkin and McWilliams, 2005; Haidvogel *et al*., 2008) coupled with a sea ice component (Danielson *et al.*, 2011). Tidal dynamics are not included in this version of the NEP model; hence tidally-forced mixing on the shelves and in the Aleutian passes is not resolved. The model domain spans 20°N to 71°N and extends approximately 2,250km offshore from the North American coast. The horizontal resolution is ~10km resulting in 212x572 grid points. There are 42 vertical levels (s-coordinate), refined for tighter spacing near the surface; these span the instantaneous thickness of water column from the sea floor to the sea surface.

The baroclinic Rossby radius in the GOA and the BS is generally smaller than 20 km (e.g. Chelton *et al*. 1998). The 10 km spatial grid and lack of tidal mixing in this modeling study are both expected to limit the resolution and/or strength of some flow features (e.g. tidal residuals, shelf-break fronts, and mesoscale eddies smaller than ~50 km), and hence to underestimate the full value of larval dispersal. Despite these limitations, we note that: 1) recent global modeling studies at ~10 km resolution without tides have still achieved very realistic results for features such as sea ice in the BS (e.g. Li *et al*. 2015a,b); and 2) a model sensitivity study of the GOA (Hermann *et al*., 2002) found that tidal information exerted a significant influence on sub-tidal scalar and velocity structure only in specific shallow areas, where the tides (and tidal mixing) are strongest. Methods used to explicitly assess our regional model's ability to hindcast observed velocities and the years selected from the hidrodynamic model are described in section 2.2.

A multi-decadal (1958–2004) simulation of currents and temperatures was conducted by E. Curchitser and K. Hedstrom (pers. comm.). Oceanic surface boundary conditions were derived from a hindcast simulation using the Community Climate System Model (CCSM; Collins *et al*., 2006) version of the Parallel Ocean Program (POP; Smith and Gent, 2002). Daily surface forcing functions (at 2°×2° resolution) were obtained from the Common Ocean-Ice Reference Experiments of Large and Yeager (2004, 2008, at http://data1.gfdl.noaa.gov/nomads/forms/mom4/COREv2.html), which consists of 6-hourly winds, air temperatures, sea level pressure and specific humidity, daily short-wave and downwelling long-wave radiation, and precipitation. Surface fluxes of heat and momentum were calculated from the atmospheric data using bulk formulae (Fairall *et al*., 1996), which include the instantaneous model sea surface temperature (SST). Freshwater runoff was applied at the coast based on spatially distributed runoff time series (T. Royer, pers. comm.) and USGS data. The oceanic surface boundary layer is computed using the K-profile parameterization (Large *et al*., 1994). The geographical northern boundary has a sink term that enforces a 0.8 Sv northward transport through the Bering Strait (Roach *et al*., 1995). Daily averages of modeled fields at 10 km resolution were archived for use in our analyses. The use of CORE atmospheric forcing excludes finer-scale atmospheric phenomena, such as those produced by local orography, in the GOA. Past sensitivity experiments using measured oceanic flux through Shelikof Strait demonstrated how increasing the resolution of the forcing winds was of limited consequence, as compared to the effect of increasing the resolution of the oceanic model itself (Hermann *et al*., 2009a). That is, many of the finer-scale ocean phenomena (e.g. observed daily flux through that narrow strait) are still reproduced adequately with the 2°×2° resolution CORE atmospheric forcing, provided the oceanic model resolution is sufficiently fine. As demonstrated below, the

use of CORE winds was adequate to capture flows through Unimak Pass, a major element of this study.

2.2 Hydrodynamic model scenarios and performance

Six runs of the hydrodynamic model were selected to be coupled with the modified IBM as indicated above.. The selection of years encompassed three years before (1978, 1982, 1988) and three years after (1992, 1999, 2001) the shift in control of recruitment dynamics of walleye pollock in the GOA characterized by an increase of juvenile pollock mortality due to a gradual build-up of groundfish predators during the mid- and late-1980s (Bailey, 2000). An IBM was run independently of the ROMS. Details of the physical model simulations and the assessment of the model's ability to reproduce observed variability and their impact in the northeast Pacific can be found in Curchitser *et al*. (2005). In addition, in this study we add some specific analysis focused in the GOA and BS to strengthen the validation within the domain of interest. Drifter data were used to explore the hydrodynamic model performance. Starting in 1986, the Alaska Fisheries Science Center (AFSC, NOAA) and Pacific Marine Environmental Laboratory (PMEL) have deployed numerous (~200) free-floating satellite-tracked Lagrangian drifters in the North Pacific Ocean and the BS. These are drogued at 25 to 40 m depth (http://www.ecofoci.noaa.gov/drifters/efoci_driftersIntro.shtml) to avoid the effect of wind on drifter movements. Our basic methodology for use of drifter data is similar to that described in Stabeno and Reed (1994). Data were readily available for years 1986-2006; hourly changes in drifter position were used to calculate the local velocity. Climatological average velocities were then derived from the drifter measurements. Model climatology was derived using 1986-2004 results of the CORE-forced hindcast. Both model and drifter data from May 15 – Oct 15 of each year were binned using the same, regular 0.5° x 0.5° latitude-longitude grid. From the data, only those bins with a total of at least 200 hourly drifter observations were retained for comparison (note that this can be from a single drifter over 200 hours or many drifters over shorter periods). Further, only those locations shallower than 200 m were compared; observations were too sparse beyond the shelf break to obtain stable mean values at the 0.5°x 0.5° resolution, due to intermittent shelf-break eddies in both model and data. Finally, using bins containing both model and data estimates, the correlation of modeled vs. observed climatological velocities was calculated separately for u and v. This approach (validation of climatological currents using bins larger than the ROMS grid itself) is intended to demonstrate the overall performance of the NEP4 model, averaged over many synoptic-scale events (storms and eddies), and covering a broad area. Pointwise validation of closely related NEP3 and NEP5 simulations has been conducted using sea surface height data (Hermann *et al*., 2009a), as well as moored current meters and temperature profiles (Hermann *et al*., 2013).

Besides model performance and model coupling, the hydrodynamic model output was used to study current patterns and transport along the domain. Some focus was put on exploring the current patterns between the GOA and BS through Unimak Pass in order to understand the connection and seasonality of the flow between both systems. Therefore, monthly mean values of the flow intensity and direction between the GOA and BS were examined. Velocities at 40 m depth were extracted from the NEP4 output, spatially averaged across Unimak Pass, and time-averaged by month for this purpose.

2.3. *Individual-based model, parameters, and mechanisms*

The IBM considers four life stages between spawning and the juvenile stage: the egg stage, the yolk-sac larval stage, the feeding larval stage, and the age-0 juvenile stage (Hinckley *et al*., 1996;

Megrey and Hinckley, 2001). Modeled processes such as growth, movement, mortality, feeding rate of larvae and bioenergetics are based on a wide variety of field and laboratory observations on this population. Egg development was driven by age and temperature (Blood *et al*., 1994). Growth of yolk-sac larvae depends on degree days, and a feeding probability is calculated to determine when larvae enter the feeding stage. The growth of feeding larvae depends on consumption estimated as a function of individual weight and temperature (Hinckley *et al*., 1996) and a bioenergetic model based on assimilation efficiency (Houde, 1989) and daily respiration rate (Yamashita and Bailey, 1989). A feeding model was also developed for juvenile pollock. This model was based on field data showing prey preference depending on juvenile walleye pollock size (M. Wilson, AFSC, Seattle, pers. comm), with an increasing shift to euphausids from copepods as juvenile fish grew. Prey availability was assumed to be constant (except where estimates were available, see below), but proportions of each type (small and large copepods, euphausids) in each area were based on historical data (M. Wilson, AFSC, Seattle, pers. comm., NPRB Project 308 Final Report). In the inner shelf areas, the density of euphausids, small copepods, and large copepods were higher (1.17838, 486.2773, 66.66362 number m^{-3}). In the mid and outer shelf and slope areas, prey densities started low (number of euphausids, small and large copepods were 0.294595, 121.56933, 16.665905 number m-3) up to Day of the Year (DOY) 120 and then increased up to DOY 160 (mid-June) to the values for the inner shelf; based on Nitrogen Phytoplankton Zooplankton model output for several years (Hinckley, 1999). Prey was set to 0 at depths >1000m (i.e. off the continental shelf). Prey consumption of juveniles was estimated using a model based on Bevelhimer and Adams (1993), Stockwell and Johnson (1997), and Stockwell and Johnson (1999). A bioenergetic model for juveniles was implemented based on Ciannelli *et al*. (1998). The digestion model implemented was based on Elliot and Pearson (1978) and uses evacuation rates for juvenile pollock (Merati and Brodeur, 1996; Mazur *et al*. 2007). The vertical position algorithm is stage-dependent as in Hinckley *et al*. (1996). Egg terminal velocity was calculated based on Sundby (1983). Yolk-sac larvae stay at hatching depth until first-feeding. Feeding larvae rise to the upper water column. At 6 mm larvae begin a type-II vertical migration (morning descent and evening ascent) with swimming speeds dependent on larval lengths. Vertical movement of juveniles is based on the calculation of a vertical mean velocity that depended on juvenile length (Hurst, 2007). A correlated random walk algorithm was added to simulate horizontal movement of juveniles (Kareiva and Shigesada, 1983). This algorithm develops a procedure to simulate movement paths as a sequence of straight lines in which juvenile displacement depended on size class. The position of the juvenile at each time step depended on the position in the previous time step, the length of the juvenile and the turning angle at each time step. Eggs, yolk-sac larvae, feeding larvae, and juveniles survival is a decreasing exponential function dependent on the instantaneous daily mortality rate at each stage (Hinckley *et al*., this issue). Groundfish predation on 0-age juveniles was added to the juvenile subroutine. Predation index was based on 8 years of groundfish predation data (K. Aydin, Alaska Fisheries Science Center, Seattle, WA, pers. Comm.). The predation index in a given year was estimated based on the consumption rate of a given predator, the estimated total biomas of the predator, and the proportion of young pollock in the diet of the predators. (Holsman and Aydin, 2015). The assumption was that the mean predation rate of 0.3 day-1 was adjusted to the mean index value and used for years when no data were available. A superindividual scheme (Scheffer *et al*., 1995; Megrey and Hinckley, 2001; Bartsch and Coombs, 2004) was added. This approach uses realistic mortality rates in IBMs by increasing the number of individuals represented by each point or float (i.e. superindividual) without greatly increasing computational times. Each particle is a superindividual that experiences mortality as the particles are tracked in time and space (Scheffer *et al*., 1995; Megrey and Hinckley, 2001). In addition, other function added was the UNESCO

equation for the estimation of seawater density based on salinity and temperature. This replaced the previous salinity linear function (Hinckley *et al*., 1996). This results in a generic model that more accurately captures seasonal changes in density. Model details and additions can be found in Hinckley *et al*. (this issue).

2.4 Spawning simulation conditions and nursery locations

Six years of the hydrodynamic model were used to accommodate interannual variability (i.e. pre and post shift in the recuritment control dynamics of pollock, cold/warm, El Niño/La Niña years) in the IBM (3 years pre and 3 years post shift) analysis to have sufficient simulation scenarios to test the spawning conditions, infer Potential Nursery Areas (PNAs), and assess retention and connectivity indices. The model domain was subdivided into 45 areas according to bathymetry and topography (islands, sounds, passes, bays, straits) to define initial spawning regions for walleye pollock, and to identify PNAs (Fig. 1). Fourteen initial areas for particle release were selected in the Eastern (ECOA), Central (CGOA), and Western Gulf of Alaska (WGOA) (white circles, Fig.1), which covered the bulk of known pollock spawning areas in the GOA (Table 1). These areas were inferred from historical data (Kendall *et al*., 1996; Matarese *et al*., 2003, Bailey *et al*., 2005), surveys of pollock egg distribution (EcoFOCI ichthyoplankton database), acoustic surveys of pollock biomass, and biological information associated with stomach contents and forage fish (Rodrigues *et al*., 2006). Given that temporal and spatial coverage of pollock egg data varied among sampling years, a historical distribution of eggs was used to define spawning grounds. This spatial distribution is consistent with the temporal integration of the recent early life retrospective analysis (fortnightly egg walleye pollock distribution) by Doyle *et al*., (this issue). Eggs were released on the 1st of each of 4 months (Feb, Mar, Apr, May) in fourteen areas (5000 in each) identified as potential spawning areas. The value of the superindividual of each egg released was proportional to the egg production estimates from the stock assessments for pollock (Dorn *et al*., 2005). A series of simulations based on life stage specific submodels where performed with varying spawning locations and timing, and years of the simulation to examine potential spatio-temporal variability in the simulated number of surviving juveniles from spawning locations. PNAs are defined as the areas of accumulation of age-0 juvenile that contain survivors at the end of the simulation. Simulated PNAs were compared with the regions where juveniles have been sampled in FOCI surveys or during NMFS acoustic surveys of the walleye pollock biomass (Table 1). In addition, the spatial distribution of the PNAs (mean surviving juvenile pollock) and the coefficient of variation (ratio of the standard deviation to the mean) were calculated to identify regions of high and low variability. Virtual individuals were tracked through space and time using a Java-based float tracking application (Lett *et al*., 2008) that uses ROMS output to compute movements. At each time step the biological submodels are resolved and individual biological properties are updated (stage, length, survival state, depth, individual vertical and horizontal velocities, horizontal position), which determine the estimates of individual movement. These diverge considerable from passive drifters and affect the calculation of retention and connectivity indices.

2.5 Retention and Connectivity matrices

Retention and connectivity indices were calculated at the end of the simulation. *Retention w*as defined as the proportion of eggs released in a particular spawning area that on the 1st of September was still in the same area. *Connectivity* is the dynamic interaction between geographically separated spawning and nursery areas via the combined effect of individual movement and currents on transport. Connectivity matrices are built based on the proportions of 0-age juveniles found on September 1st in a specific nursery area that come from each spawning

ground. Given the complexity of the connectivity matrices and varying factors, the connectivity matrices among 45 PNAs were aggregated, after the simulation, into broader 'sectors' (Fig.1) to simplify the model output interpretation. Note that lumping spawning areas before the model simulations would result in a loss in spatial resolution impacting transport patterns, connectivity, retention and subsequent interpretations. To summarize connectivity patterns, results were aggregated by three spawning sectors (EGOA, CGOA and WGOA) and eight nursery sectors (EGOA, CGOA, WGOA, AL, EBS, WBS, Arctic (AR) and the GOA Basin (BAS)).

3. Results and discussion

3.1 Hydrodynamic model performance

Model runs from ROMS NEP4 were analyzed and compared with velocities inferred from drift data. Specifically, modeled currents integrated between 15 May and 15 of October for the modeled years (1986 to 2004) were compared with Eulerian velocities generated through the spatial discretization of satellite drifter data released in the GOA and BS for the same period (Fig. 2). Although model and data do not have the same coverage, the data partially cover the CGOA, WGOA, BS Middle (Areas 30, 34 and 38; Fig. 1) and Outer (Areas 31, 35 and 39; Fig.1) domains. Overall, the intensity and the direction of the modeled currents are consistent with the intensity and direction of the observed currents. A scatterplot comparing measured and modeled u and v velocities shows good agreement between simulated and observed velocity components (Fig.3) with coefficients of determination (R^2) of 0.5 for the u-component and 0.63 for the v component. Detailed evaluation of the hydrodynamic model used in this study is presented in Curchitser *et al*. (2010), Danielson *et al*. (2011), and Cheng *et al*. (2014). The consensus was that sea ice cover was generally well represented in the model for the Bering Sea, and model kinetic energy was similar to empirical observations at frequencies lower than three days and at tidal frequencies. Sampled transects from model output showed that the model reproduced seasonal water column transitions from a well-mixed shelf regime, to a highly stratified two-layer system during the summer at the mid-shelf. The near-shore remained well mixed throughout the year in the empirical data and in the model results, with energy for mixing supplied from both wind and tide forcing. In addition, characteristic oceanographic features of the GOA and the BS (Stabeno and Reed, 1994; Stabeno *et al*. 2004) are observed in the modeled time-averaged velocities (March through September) for the years of the simulation (Fig.A1 appendix). Modeled velocities on the shelf exhibit a southwest current along the Alaska Peninsula toward the AL. Low current intensities (<0.04 m/s) are observed in Cook Inlet, Prince William Sound, north, south and west of Kodiak Island, in bays along the Alaska Peninsula, and in the Shumagin Islands region (Fig.1). Eddies are produced beyond the shelf break in the Alaskan Stream (e.g. note deformation of the Alaskan Stream around an eddy at 57°N, 150°W in Fig. A1(a) appendix). A consistent flow into the BS through Unimak Pass and other Aleutian passes is showed in the simulations (Fig.A1 appendix). The average monthly flow through Unimak Pass calculated for the first 40 m showed a consistent flow from the GOA through Unimak Pass to the BS in all years of the simulation (Fig.4). The climatological mean over all simulation years shows that the flow through Unimak Pass to the BS intensifies from September to January of the following year, decaying toward August. However, interannual variability is high. The speeds and seasonal pattern correspond to the measurements of Stabeno *et al*. (2002). The modeled flow between March and September from the CGOA and towards the AL is consistent with that observed in binned, time-integrated velocities. Potential limitations of this model compared to other recent ocean model configurations (Dobbins *et al*., 2009; Coyle *et al*., 2012; Gibson *et al*., 2013) have been raised by Hinckley *et al*. (this issue).

3.2 Biophysical model performance and known nursery areas in GOA

The coupled biophysical IBM was used to examine connections between potential spawning and nursery areas, and how the relative strength of these connections varied over the spawning season. Historically, the majority of pollock spawning in the GOA occurred from mid-March to early May in Shelikof Strait (Fig. 1, Kendall *et al*., 1987; Schumacher and Kendall, 1991), with peak spawning at the start of April in the deepest part of Shelikof Strait. After spawning, eggs and larvae are advected southwest by the Alaska Coastal Current along the Alaska Peninsula and arrive in the Shumagin Islands 8 to 10 weeks later. Eggs and larvae may also be advected into the Alaskan Stream, where they can be lost from the population (Bailey *et al*., 1999). The Shumagin Islands region has traditionally been considered the nursery area that ensures the success of the population in the GOA (Hinckley *et al*., 1991, Wilson *et al*., 1996). Our results showed a high mean density of surviving (simulated) juvenile pollock (integrated over years) occurring primarily in the Shumagin Islands area (Fig.5a corresponding to areas 17 and 18; see Fig.1) which presented the lowest coefficient of variation (Fig.5b). In addition, model results confirmed a strong link between the Shelikof Strait spawning area and the Shumagin nursery region with 40-45% connectivity for March spawners and 45-50% for April spawners (Fig.A2 appendix). Model simulations demonstrated that destinations of surviving age-0 walleye pollock agreed with the observed nursery area, which extends from the Semidi Islands to Unimak Pass (Brodeur and Wilson, 1996; Wilson *et al*., 1996; Wilson, 2000). Additional observations of juveniles near the coast of the Alaska Peninsula inshore of Shumagin Island (Hinckley *et al*., 1991; Brodeur *et al*., 1995; Wilson *et al*., 1996; Hinckley *et al*., this issue) support this claim. Other simulated PNAs included the Semidi Islands (SemI), coastal Aleutian Islands (UI and UIof) and northeast of Kodiak Island (Oc, Kin and KIS) (Fig.5a), which are consistent with known or suspected nursery regions described in the literature (Table 1). Supporting evidence for the importance of the Semidi Islands as a juvenile walleye pollock nursery area is derived from a spatial bioenergetics model for the western GOA, which indicated that habitat conducive to juvenile walleye pollock growth was located along the eastern edge of Semidi Bank, in the vicinity of Castle Cape, Kupreanof Point, and south-west of Sutwik Island (Fig.1, Mazur *et al*., 2007). Fish spawned in the North Kodiak area were transported to the southwest GOA, to the BS, and to the AL regions. A potential caveat to this result is that juvenile fish found in bays around northern and eastern Kodiak Island (Wilson *et al*., 1996) may have been spawned on the continental shelf near Kodiak Island, and may exhibit behavior and directed swimming not modeled in the IBM. The ROMS, which uses a 10 km grid, does not accurately resolve flow into and out of coastal bays. Consequently, we cannot determine the use of coastal bays as nursery areas at this time. Statistical evaluation of the ability of the walleye pollock biophysical model to reproduce observed distributions of early larvae and juvenile walleye pollock (Hinckley *et al*., this issue) increases the credibility of using IBMs to understand pollock early life history.

3.3 Model projections: Retention and connectivity in GOA and links to BS and surrounding areas

In our simulation the most prominent GOA PNAs were to a large extent characterized by a high retention level. The maximum mean retention of age-0 juvenile walleye pollock, integrated through time by September 1st, was 0.28 in the Shumagin Islands Inner area (SIin). This was followed by Prince William Sound Inner area (PWSin) and Outer Cook Inlet (OC) area with retention proportions of 0.22 (Fig. 6a). Eggs spawned in February had the lowest proportion of retention, while those spawned in May had the highest retention with the exception of SIin where the highest retention is reached in April (Fig. 6b). This is consistent with what has been observed and hypothesized about pollock larvae. Several retention mechanisms have been proposed in GOA: larvae after spawning can be transported onshore, trapped in meanders of weaker or

reversed flow or entrained in eddies (Bailey *et al*., 1995; Bailey *et al*., 1997; Bograd *et al*., 1994; Hinckley *et al*., 1991; Shumacher and Kendall, 1991; Shumacher *et al*., 1993). These mechanisms can increase larval residence time and retention, and lessen their chances to be advected offshore. In addition, in the model, retention is a function of physical forcing, the ability to self-locomote, as well as, the temperature that affect development and growth of early stages and the timing on reaching self movement. Therefore, high retention will be factored for all these processes together. Concerning connectivity, an interesting finding of this study was that the BS can be an important nursery area for several spawning grounds located in the GOA. The simulations showed the highest density of surviving pollock (simulated, Fig. 5a) in the outer domain of the WBS (areas 31, Fig.1) followed by the western regions of WBS (areas 32 and 36; Fig.1). From these PNAs, the lowest coefficients of variation were associated with the outer domain of the WBS (Fig. 5b), except for area 31 (BSSo) and the eastern portion of area 32 (BSSb; Fig.1). Monthly variability of spawning affected survival, with transport into the BSSb area (the highest density of surviving pollock; Fig.7) increasing among eggs released up to April and then decreasing in May. Transport to the BSSo area increased for spawning occurring from February to May, while the opposite pattern was observed in BSCm and BSCb (Fig.7). Simulated walleye pollock spawned during February in the Shumagin Islands were transported to the BS, with few retained in this region (Shumagin Islands, Fig. A2 appendix). There is evidence that walleye pollock spawning locations have shifted in recent years, and additional spawning areas (Unimak Pass, Semidi and Shumagin Islands) have been described (Ciannelli *et al*., 2007). As an example, recent acoustic surveys have observed concentrations of spawning fish in the Shumagin Islands (Dorn *et al*., 2013). Little is known about the fate of walleye pollock spawned in this region (Dorn *et al*., 2013). Our model showed that the average transport through Unimak Pass (~0.5 Sv), the mechanism linking the GOA and BS, is consistent with values found in Stabeno *et al*. (2002), leading to the conclusion that it is unlikely that the physical model overestimated flow to the BS. Other studies also support this mechanism of connection between the GOA and BS (Gibson *et al*., 2013). The analysis of the connectivity matrix integrated by sectors showed strong retention within the GOA. High retention is observed in the CGOA (25.9%) and EGOA (23.8%), while the WGOA showed only 7.2% retention (Table 2). Within the GOA, the highest connectivity is observed from the EGOA to the CGOA (57.8%) followed by the connection from the CGOA to the WGOA (24.3%). Overall, the most prominent connections were the ones found between sectors in the GOA and the BS, such as the connectivity from the WGOA to the WBS (62.8%) and from the CGOA to the WBS (29.2%, Table 2). Based on these spawning and nursery connectivity matrices, four hypothetical spawning scenarios for the GOA were built to better understand the contribution of different spawning scenarios to PNAs, and the connectivity to regions out of the GOA (Fig.8):

Scenario A: Spawning occurs in the EGOA sector (Fig.8, upper left). Under this scenario, close to 93% of eggs spawned in EGOA stays in the GOA, with the remainder transported to the BS (3%) and the AL (4%).
Scenario B: Spawning occurs in CGOA sector (Fig.8, upper right). Only 50% of eggs spawned in the CGOA stay in the GOA, with moderate retention in the CGOA. The remaining survivors have nursery grounds in the BS (35%), in the AL (12%) and in the BAS (3%).
Scenario C: Spawning occurs in WGOA sector (Fig. 8, lower left). Only 7% of eggs spawned in the WGOA stays in the GOA. The majority of eggs end up in nursery grounds in the BS (81%), some in the AL (7%), and a small percentage in the AR (2%).
Scenario D: All spawning sectors combined. The overall mean connectivity from the model predicts that 40% of surviving juveniles spawned in the GOA are exported to the BS (mainly to

WBS and secondarily to EBS, see Table 2) and 50% are retained in the GOA (mainly in the CGOA and secondarily in the WGOA). The remaining juveniles are exported to the AL (7.5%), the AR (0.5), and the BAS (2%).

Our results of modeled scenarios A (only EGOA) and B (only CGOA) suggest that spawning in the EGOA and CGOA sectors promote retention of juveniles in the GOA. Scenario C (only WGOA) is the one that showed the strongest connectivity with the BS (EBS and WBS). Scenarios B, C and D (all spawning combined) suggest that GOA spawning success and transport rates may be influencing walleye pollock recruitment in the BS, especially in cases when spawning occurs in the WGOA, a sector that is highly connected to the WBS and secondarily to the EBS. It is important to note that recruitment will depend on the relative sizes of the spawning biomass in the EBS, AL and GOA. Various possible outcomes can occur when larvae and juvenile are transported to the BS. If surviving GOA juveniles in the BS develop, grow, and recruit to the BS fishery, then transport of individuals to the BS influences walleye pollock cohort strength in both the GOA and the BS. The impact of this emigration may not be large on the BS walleye pollock population as the BS pollock stock is an order of magnitude larger than the GOA stock. Survival rates of GOA pollock in the BS may also be low, given that juvenile pollock in the BS (age-1's and 2's) tend to be observed in waters of the northern BS (i.e., west of 170°, (Honkalehto *et al*., 2013). BS walleye pollock originating in the GOA would have to run the gauntlet of cannibalistic pollock and increasing numbers of arrowtooth flounder (*Atheresthes stomias*) that are found in the GOA and in the southern half of the Bering Sea (Turnock *et al*., 2005). There is also the possibility that GOA walleye pollock juveniles that initially settled in the BS may return to the GOA as pre-recruits or adult fish. At the current state, the IBM only simulates egg through age-0 juvenile life history stages. Despite GOA spawned pollock transported to ay may stay in the B, there is uncertainty whether that fish will two years later recruit to the commercial fishery.

Mixing of pollock larvae spawned in the GOA and BS might occur particularly over the Middle and Outer Domains of the BS continental shelf, although the influx would be extremely low relative to larvae of BS origin (Batchelder *et al*., 2010). Our simulation results showed strong connections between the WGOA and BS, which are supported by other studies that have suggested that eggs and larvae may be advected into the BS through Unimak Pass, a potential conduit for exchange between the GOA and the BS (Lanksbury *et al*., 2007; Duffy-Anderson *et al*., in press). This might suggest a metapopulation structure for pollock in Alaska. In contrast, studies indicate genetic differentiation among pollock in the GOA and BS. However, genetic differences appear between broad regions, but resolution between adjacent stocks is lacking (Bailey *et al*., 1999), and the boundaries between regional stocks are poorly defined (Grant el at., 2010). A shift in pollock spawning locations to the WGOA sector such as Unimak Pass, Semidi and Shumagin Islands (which is strongly connected with the BS in the model), have been recently described (Ciannelli *et al*., 2007). Genetic differences between populations, prompted under the response of subpopulation contraction-expansion to environmental variability (Grant *et al*., 2010) and/or spawning shifts, do not accumulate on small spatial and temporal scales. Although speculative, larval drift mechanisms operating in the recently described shifted spawning areas in the WGOA might lead to incipient homogenization of the stock in the GOA-BS boundary, at a scale at which genetics are not sensitive yet. Future studies should incorporate realistic initial spawning conditions such as Doyle *et al*. (this issue), and explore interannual variability in spawning location on connectivity. Understanding the effects of this variability on transfers between spawning and nursery areas would provide insight to local and metapopulation

dynamics, community structure, and genetic diversity (Hastings and Harrison, 1994), and can be used to evaluate and design resource management strategies.

Acknowledgements
We thank the North Pacific Research Board for funding Project 523: Pollock recruitment and stock structure, which supported portions of this research. We would also like to acknowledge support from the EcoFOCI group and the RACE Division at the Alaska Fisheries Science Center, which provided data, personnel salaries, and other support. We thank Dr. Andre Punt who provided numerous insightful comments which lead to an important improvement of the manuscript. We thank deeply the anonymous reviewers for their constructive feedback and insightful suggestions which allowed us to improve the manuscript.

References
Bacheler, N.M., Ciannelli, L., Bailey, K.M., and Duffy-Anderson, J.T. 2010. Spatial and temporal patterns of walleye pollock (*Theragra chalcogramma*) spawning in the eastern Bering Sea inferred from egg and larval distributions. Fisheries Oceanography 19(2):107–120.

Bailey, K. M., Canino, M. F., Napp, J. M., Spring, S. M., and Brown, A. J. 1995. Contrasting years of prey levels, feeding conditions and mortality of larval walleye pollock *Theragra chalcogramma* in the western Gulf of Alaska. Marine Ecology Progress Series 119:11-23.

Bailey, K.M., Stabeno, P.J. and Powers, D.A. 1997. The role of larval retention and transport features in mortality and potential gene flow of walleye pollock. Journal of Fish Biology 51(Suppl. A):135-154.

Bailey, K.M., Bond, N.A. and Stabeno, P.J., 1999. Anomalous transport of walleye pollock larvae linked to ocean and atmospheric patterns in May 1996. Fisheries Oceanography 8:264-273.

Bailey, K.M. 2000. Shifting control of recruitment of walleye pollock *Theragra chalcogramma* after a major climatic and ecosystem change. Marine Ecology Progress Series 198:215-224.

Bailey, K. M., Ciannelli, L., Bond, N.A., Belgrano, A. and Stenseth, N. C. 2005. Recruitment of walleye pollock in a physically and biologically complex ecosystem: A new perspective. Progress in Oceanography 76:24-42.

Bartsch, J., and Coombs, H., 2004. An individual-based model of the early life history of mackerel *(Scomber scombrus*) in the eastern North Atlantic, simualting transport, growth and mortality. Fisheries Oceanography 13(6):365-379.

Beck, M.W., Heck, K.L., Able, K.W. Jr., Childers, D.L., Eggleston, D.B., Gillanders, B.M., Halpern, B., Hays, C.G., Hoshino, H., Minello, T.J., Orth, R.J., Sheridan, P.F., and Weinstein, M.P. 2001. The identification, conservation, and management of estuarine and marine nurseries for fish and invertebrates. BioScience 51: 633-641.

Bevelhimer, M.S., and Adams, S.M. 1993. A bioenergetic analysis of diel vertical migration by kokanee salmon, *Oncorhynchus nerka*. Canadian Journal of Fisheries and Aquatic Science 50:2336-2349.

Blood D.M., Matarese, A.C., and Yoklavich, M.M., 1994. Embryonic development of walleye pollock *Theragra chalcogramma*, from Shelikof Strait, Gulf of Alaska. Fisheries Bulletin US, 92:207-222.

Botsford L.W., Hastings, A. and Gaines, S.D. 2001. Dependence of sustainability on the configuration of marine reserves and larval dispersal distance. Ecology Letters 4:144-150.

Brodeur, R.D., Busby, M.S. and Wilson, M.T. 1995. Summer distribution of early life stages of walleye pollock, *Theragra chalcogramma*, and associated species in the western Gulf of Alaska. Fishery Bulletin 93: 603-618.

Brodeur, R.D., and Wilson, M.T. 1996. A review of the distribution, ecology and population dynamics of age-0 walleye pollock (*Theragra chalcogramma*) in the Gulf of Alaska. Fisheries Oceanography 5 (1):148-166.

Chelton, D. B., deSzoeke, R.A., Schlax, M.G., El Naggar, K. and Siwertz, N., 1998: Geographical variability of the first-baroclinic Rossby radius of deformation. Journal of Physical Oceanography 28: 433-460.

Cheng, W., Curchitser, E.N., Stock, C., Hermann, A.J., Cokelet, E., Mordy, C., Stabeno, P., Hervieux, G. and Castruccio, F. 2014. What processes contribute to the spring and fall bloom co-variability on the Eastern Bering Sea shelf? Deep-Sea Research II (In rev).

Ciannelli, L., Brodeur, R.D., Buckley, T.W., 1998. Development and application of a bioenergetics model for juvenile walleye pollock. Journal of Fish Biology 52: 879–898.

Ciannelli, L., Bailey, K.M., Chan, K., and Stenseth, N.C. 2007. Phenological and geographical patterns of walleye pollock (*Theragra chalcogramma*) spawning in the western Gulf of Alaska. Canadian Journal of Fisheries and Aquatic Science 64: 713-722.

Collins, W.D., Bitz, C.M., Blackmon, M.L., Bonan, G.B., Bretherton, C.S., Carton, J.A., Chang, P., Doney, S.C., Hack, J.J., Henderson, T.B., Kiehl, J.T., Large, W.G., McKenna, D.S., Santer, B.D., Smith, R.D., 2006. The Community Climate System Model Version 3 (CCSM3). Journal of Climate 19:2122–2143.

Cooper, D.W., Duffy-Anderson, J.T., Stockhausen, W.T., and Cheng, W. 2013. HYPERLINK "http://www.pmel.noaa.gov/public/pmel/publications-search/search_abstract.php?fmContributionNum=3773"Modeled connectivity between northern rock sole (*Lepidopsetta polyxystra* HYPERLINK "http://www.pmel.noaa.gov/public/pmel/publications-search/search_abstract.php?fmContributionNum=3773") spawning and nursery areas in the eastern Bering Sea. Journal of Sea Research 84, doi: 10.1016/j.seares.2012.07.001, 2–12.

Cowen R.K., Lwiza K.M.M., Sponaugle S., Paris C.B. and Olson D.B. 2000. Connectivity of marine populations: Open or closed? Science 287:857-859.

Cowen, R.K. 2002. Larval dispersal and retention and consequences for population connectivity. In: Coral reef fishes. Dynamics and diversity in a complex ecosystem, P. F. Sale, editors, Academic Press, San Diego, pp. 149-170.

Cowen R.K., Gawarkiewicz G., Pineda J., Thorrold S.R. and Werner F. 2007. Population connectivity in marine systems. An overview. Oceanography 20:14-21.

Cowen, R.K., and Sponaugle, S. 2009. Larval dispersal and marine population connectivity. Annual Review of Marine Science 1:443-466.

Coyle, K., Cheng, W., Hinckley, S.L., Lessard, E.J., Whitledge, T., Hermann, A.J. and Hedstrom, K. 2012. Model and field observations of effects of circulation on the timing and magnitude of nitrate utilization and production on the northern Gulf of Alaska shelf. Progress in Oceanography, 103:16-41.

Curchitser, E.N, Haidvogel, D.B., Hermann, A.J., Dobbins, E.L., Powell, T. and Kaplan, A. 2005. Multi-scale modeling of the North Pacific Ocean: Assessment of simulated basin-scale variability (1996-2003). Journal of Geophysical Research 110: C11021, doi:101029/2005JC002902.

Curchitser, E.N., Hedstrom, K., Danielson, S. and Weingartner, T.J. 2010. Modeling of circulation in the North Aleutian Basin, OCS Study BOEMRE 2010-028, Bureau of Ocean Management., U.S. Department of the Interior, Washington, D. C. [Available at http://alaska.boemre.gov/reports/2010rpts/2010_028.pdf.]

Danielson, S., Curchitser, E., Hedstrom, K., Weingartner, T. and Stabeno, P. 2011. On ocean and sea ice modes of variability in the Bering Sea. Journal of Geophysical Research 116, C12034 doi:10.1029/2011JC007389.

Dobbins, E.L., Hermann, A.J., Stabeno, P.J., Bond, N.A., and Steed, R.C. 2009. Modeled transport of freshwater from a line-source in the coastal Gulf of Alaska. Deep Sea Research II,doi:10.1016/j.dsr2.2009.02.004.

Dorn, M., Aydin, K., Barbeaux, S., Guttormsen, M., Megrey, B., Spalinger, K. and Wilkins, M. 2005. Assessment of walleye pollock in the Gulf of Alaska In: Appendix B. Stock assessment and fishery evaluation report for the groundfish resources of the Gulf of Alaska, North Pacific Fishery Management Council, P.O. Box 103136, Anchorage, AK 99510.

Dorn, M.W., Aydin, K., Barbeaux, S., Jones, S., Spalinger, K., and Palsson, W. 2012. Assessment of the walleye pollock stock in the Gulf of Alaska. In Stock Assessment and Fishery Evaluation Report for Groundfish Resources of the Gulf of Alaska. Prepared by the Gulf of Alaska Groundfish Plan Team, North Pacific Fishery Management Council, P.O. Box 103136, Anchorage, AK 99510. North Pacific Fisheries Management Council, Anchorage, AK.

Dorn, M.W., Aydin, K., Barbeaux, S., Jones, S., Palsson, W., and Spalinger, K. 2013. Assessmentof the walleye pollock stock in the Gulf of Alaska. In Stock Assessment and Fishery Evaluation Report for Groundfish Resources of the Gulf of Alaska. Prepared by the Gulf of Alaska Groundfish Plan Team, North Pacific Fishery Management Council, P.O. Box 103136, Anchorage, AK 99510. North Pacific Fisheries Management Council, Anchorage, AK.

Dorn, M.W., Aydin, K., Jones, D., Spalinger, K. and Palsson, W. 2014. Assessment of the walleye pollock stock in the Gulf of Alaska. In Stock Assessment and Fishery Evaluation Report for Groundfish Resources of the Gulf of Alaska. Prepared by the Gulf of Alaska Groundfish Plan Team, North Pacific Fishery Management Council, P.O. Box 103136, Anchorage, AK 99510. North Pacific Fisheries Management Council, Anchorage, AK.

Doyle, M. and Mier, K. (this issue). Pelagic early life history exposure profiles of selected commercially important fish species in the Gulf of Alaska. Deep Sea Research II.

Duffy-Anderson, J.T., Blood, D.M., Cheng, W., Ciannelli, L., Materese, A.C., Sohn, D., Vance, T.C. and Vestfals, C. 2013. HYPERLINK "http://www.pmel.noaa.gov/public/pmel/publications-search/search_abstract.php?fmContributionNum=3800"Combining field observations and modeling approaches to examine Greenland halibut (*Reinhardtius hippoglossoides*) early life ecology in the southeastern Bering Sea. Journal of Sea Research 75, doi: 10.1016/j.seares.2012.06.014, 96–109.

Duffy-Anderson, J.T., Doyle, M., Mier, K. and Stabeno, P. Early life ecology of Alaska plaice (*Pleuronectes quadrituberculatus*) in the eastern Bering Sea: seasonality, distribution, and transport pathways. Journal of Sea Research (in press).

Elliott, J. M., and Pearson, L. 1978. The estimation of daily rates of food consumption for Fish Journal of Animal Ecology 47: 977-991.

Fairall, C.W., Bradley, E.F. Rogers, D.P. Edson, J.B. and Young, G.S. 1996. Bulk parameterization of air-sea fluxes for Tropical Ocean-Global Atmosphere Coupled-Ocean Atmosphere Response Experiment. Journal of Geophysical Research 101(C2):1295-1308.

Gaines S.D., Caylord B., Gerber L.R., Hastings A. and Kinlan B.P. 2007. Connecting places. The ecological consequences of dispersal in the sea. Oceanography 20: 90-99.

Gibson, G.A., Coyle, K.O., and Curchister, E. 2013. A modelling study to explore on-shelf transport of oceanic zooplankton in the Eastern Bering sea. Journal of Marine Systems 121-122:47-64.

Grant, W.S. and Utter, F.M. 1980. Biochemical genetic variation in walleye pollock, *Theragra chalcogramma*: population structure in the southeastern Bering Sea and the Gulf of Alaska. Canadian Journal of Fisheries and Aquatic Sciences 37:1093–1100.

Grant, W.S., Spies, I., and Canino, M.F. 2010. Shifting-balance stock structure in North Pacific walleye pollock (Gadus chalcogrammus). ICES Journal of Marine Science 67: 1687-1696.

Haidvogel, D.B., H. Arango, W.P. Budgell, B.D. Cornuelle, E. Curchitser, E. Di Lorenzo, K. Fennel, W.R. Geyer, A.J. Hermann, L. Lanerolle, J. Levin, J.C. McWilliams, A.J. Miller, A.M.

Hastings, A. and Harrison, S. 1994. Metapopulation dynamics and genetics. Annual Review of Ecology and Systematics, 25: 167-188.

Hermann, A.J., Stabeno, P.J., Haidvogel, D.B., and Musgrave, D.L. 2002. A regional tidal/subtidal circulation model of the southeastern Bering Sea: Development, sensitivity analyses and hindcasting. Deep-Sea Research II 49: 5495-5967.

Hermann, A. J., Curchitser, E.N., Haidvogel, D.B. and Dobbins, E.L. 2009a. A comparison of remote versus local influence of El Nino on the coastal circulation of the northeast Pacific. Deep Sea Research II 56: 2427–2443.

Hermann, A.J., Hinckley, S., Dobbins, E.L., Haidvogel, D.B., Bond, N.A., Mordy, C., Kachel, N. and Stabeno, P.J. 2009b. Quantifying cross-shelf and vertical nutrient flux in the Gulf of Alaska with a spatially nested, coupled biophysical model. Deep Sea Research II 56: 2474–2486.

Hermann, A. J., G. A. Gibson, N. A. Bond, E. N. Curchitser, K. Hedstrom, W. Cheng, M. Wang, P. J. Stabeno, L. Eisner, K. D. Cieciel. 2013. A multivariate analysis of observed and modeled biophysical variability on the Bering Sea shelf: multidecadal hindcasts (1970-2009) and forecasts (2010-2040). Deep Sea Research IIDeep-Sea Res. II 94, doi: HYPERLINK "http://www.sciencedirect.com/science/article/pii/S096706451300146X"10.1016/j.dsr2.2013.04.007, 121-139.

Hermann, A. J., Gibson, G.A., Bond, N.A., Curchitser, E.N., Hedstrom, K., Cheng, W., Wang, M., Cokelet, E.D., and Stabeno, P.J.. This issue. Projected future biophysical states of the Bering Sea. Submitted to Deep-Sea Research II.

Hinckley, S., Bailey, K.H., Picquelle, S.J., Shumacher, J.D. and Stabeno, P.J., 1991. Transport, distribution, and abundance of larval and juvenile walleye pollock (*Theragra chalcogramma*) in the western Gulf of Alaska. Canadian Journal of Fisheries and Aquatic Sciences 48: 91-98.

Hinckley, S., Hermann, A.J. and Megrey, B.A. 1996. Development of a spatially explicit, individual-based model of marine fish early life history. Marine Ecology progress series 139: 47-68.

Hinckley, S. 1999. Biophysical mechanisms underlying the recruitment process in walleye pollock (*Theragra chalcogramma*). PhD dissertation, University of Washington, Seattle. 258 pp.

Hinckley, S., Hermann, A.J., Mier, K. and Megrey, M. 2001. Importance of spawning location and timing to successful transport to nursery areas: a simulation study of Gulf of Alaska walleye pollock. ICES Journal of Marine Sciences 58: 1042-1052.

Hinckley, S., Parada, C., Horne, J., Hermann, A.J., Megrey, B. and Dorn, M. 2008. Walleye Pollock Recruitment and Stock Structure in the Gulf of Alaska: An investigation using a suite of biophysical and individual-based models. Report: North Pacific Research Board Project 523, Final Report, 108 pages [Available at HYPERLINK "http://doc.nprb.org/web/05_prjs/523_Final Report_July2010.pdf"http://doc.nprb.org/web/05_prjs/523_Final%20Report_July2010.pdf].

Hinckley, S., Parada, C., Horne, J.K. and M. Mazur (this issue). Comparison of individual-based model output to data using a model of walleye pollock early life history in the Gulf of Alaska. Deep-Sea Research II. (This is)

Holsman, K.K., and Aydin, K. 2015. Comparative methods for evaluating climate change impacts on the foraging ecology of Alaskan groundfish. Marine Ecology Progress Series 521: 217–23.
.
Honkalehto, T., McCarthy, A, Ressler, P., and Jones, D. 2013. Results of the acoustic-trawl survey of walleye pollock (*Theragra chalcogramma*) on the U.S. and Russian Bering Sea Shelf in June - August 2012 (DY1207). AFSC Processed Rep. 2013-02, 60 p. Alaska Fish. Sci. Cent., NOAA,Natl. Mar. Fish. Serv., 7600 Sand Point Way NE, Seattle WA 98115.

Houde, E.D., 1989. Comparative growth, mortality, and energetic of marine larvae: temperature and implied latitudinal effects. Fishery Bulletin US 87: 471-495.

Hurst, T. 2007. Thermal effects on behavior of juvenile walleye Pollock (*Theragra chalcogramma*): implications for energetics and food web models. Canadian Journal of Fisheries and Aquatic Science 64: 449-457.

Kareiva, P.M. and Shigesada, N., 1983. Analyzing insect movement as a correlated random walk. Oecologia 56: 234-238.

Kendall, A.W. Jr, Clarke, M.E., Yoklavich, M.M. and Boehlert, G.W. 1987. Distribution, feeding, and growth of larval walleye pollock, *Theragra chalcogramma*, from Shelikof Strait,
Gulf of Alaska. Fishery Bulletin US 85: 499-521.

Kendall, A.W., Incze, Jr., L.S., Ortner, P.B., Cummings S.R., and Brown, P.K. 1994. The vertical distribution of eggs and larvae of walleye pollock, *Theragra chalcogramma*, in Shelikof Strait, Gulf of Alaska. Fishery Bulletin 92: 540-554.

Kim, S-S, Moon, D-Y. and Yang, W-S. 2000. Mitochondrial DNA analysis for stock identification of walleye pollock, *Theragra chalcogramma*, from the North Pacific Ocean. Bulletin of National Fisheries Research and Development Agency (Korea) 58:22 27.

Lanksbury, J.A., Duffy-Anderson, J.T., Busby, M., Stabeno, P.J. and Mier, K.L. 2007. Abundance and distribution of northern rock sole (*Lepidopsetta polyxystra*) larvae in relation to oceanographic conditions in the Eastern Bering Sea. Progress in Oceanography 72:39–62.

Large, W., McWilliams, J. and Doney, S. 1994. Oceanic vertical mixing: A review and a model with a nonlocal boundary layer parameterization, Reviews in Geophysics 32: 363-403.

Large, W. and Yeager, S. 2004. Diurnal to decadal global forcing for ocean and sea-ice models: the data sets and flux climatologies. CGD Division of the National Center for Atmospheric Research, NCAR Technical Note: NCAR/TN-460+STR.

Large, W. and Yeager, S.G. 2008. The global climatology of an interannually varying air-sea flux data set. Climate Dynamics 33: 341–364.

Largier, J. L., 2003. Considerations in estimating larval dispersal distances from oceanographic data. Ecological Applications 13(1):S71-S89.

Lett, C., Verley, P., Mullon, C., Parada, C., Brochier, T., Penven, P. and Blake, B. 2008. A Lagrangian tool for modeling ichthyoplankton dynamics. Environmental Modelling Software 23: 1210-1214.

Li, L., McClean, J., Miller, A., Eisenman, I., Hendershott, M., and Papadopoulos, C., 2014a. Processes driving sea ice variability in the Bering Sea in an eddying ocean/sea ice model: Mean seasonal cycle, Ocean Modelling 84: doi: 10.1016/j.ocemod.2014.09.006,51-66.

Li, L., Miller, A., McClean, J., Eisenman, I., and Hendershott, M., 2014b. Processes driving sea ice variability in the Bering Sea in an eddying ocean/sea ice model: Anomalies from the mean seasonal cycle, Ocean Dynamics 64: doi:10.1007/s10236-014-0769-7.1693-1717.

Matarese, A.C., Blood, D.M., Picquelle, S.J., and Benson, J.L.. 2003. Atlas of abundance and distribution patterns of ichthyoplankton from the northeast Pacific Ocean and Bering Sea ecosystems based on research conducted by the Alaska Fisheries Science Center (1972-1996). NOAA Prof. Paper NMFS 1, 281 p.

Mazur, M.M., Wilson, M.T., Dougherty, A.B., Buchheister, A. and Beauchamp, D.A. 2007. Temperature and prey quality effects on growth of juvenile walleye pollock *Theragra chalcogramma*: a spatially explicit bioenergetics approach. Journal of Fish Biology 70: 816-136.

Megrey, B.A. and Hinckley, S. 2001. Effect of turbulence of larval fishes: a sensitivity analysis using an individual-based model. ICES Journal of Marine Sciences 58: 1015-1029.

Merati, N., and Brodeur, R.D. 1996. Feeding habits and daily ration of juvenile walleye pollock, Theragra chalcogramma, in the western Gulf of Alaska. In Ecology of juvenile walleye pollock, Theragra chalcogramma (Brodeur, R. D., Livingston, P. A., Loughlin, T. R., Hollowed, A. B. eds), pp.65-79. U.S. Department of Commerce, NOAA Technical Report NMFS 126.

Mulligan, T.J., Chapman, R.W. and Brown, B.L. 1992. Mitochondrial DNA analysis of walleye pollock, *Theragra chalcogramma*, from the eastern Bering Sea and Shelikof Strait, Gulf of Alaska. Canadian Journal of Fisheries and Aquatic Sciences 49:319–326.

North, E.W., Gallego, A. and Petitgas, P. 2009. Manual of recommended practices for modeling physical-biological interactions during fish early life. ICES Coop. Res.Rep. No. 295.

Olsen, J.B., Merkouris, S.E. and Seeb, J.E. 2002. An examination of spatial and temporal genetic variation in walleye pollock (*Theragra chalcogramma*) using allozyme, mitochondrial DNA, and microsatellite data. Fishery Bulletin 100:752–764.

O'Reilly, P.T., Canino, M.F., Bailey., K.M. and Bentzen, P. 2004. Inverse relationship between FST and microsatellite polymorphism in the marine fish, walleye pollock (*Theragra chalcogramma*): implications for resolving weak population structure. Molecular Ecology 13:1799–1814.

Pineda J., Hare, J. and Sponaugle, S.U. 2007. Larval transport and dispersal in the coastal ocean and consequences for population connectivity. Oceanography 20: 22-39.

Roach, A.T., Aagaard, K., Pease, C.H., Salo, S.A., Weingartner, T., Pavlov., V. and Kulakov, M. 1995. Direct measurements of transport and water properties through Bering Strait. Journal of Geophysical Research 100(18): 443–457.

Rodrigues, R., Nemeth, M., Markowitz, T. and Funk, D. 2006. Review of literature on fish species and beluga whales in Cook Inlet, Alaska. Final report prepared by LGL Alaska Research Associates, Inc., Anchorage, AK, for DRven Corporation, Anchorage, AK.

Sale, P.F., Cowen, R.K., Danilowicz, B.S., Jones, G.P., Kritzer, J.P., Lindeman, K.C., Planes, S., Polunin, N.V.C., Russ, G.R., Sadovy, Y.I. and Steneck, R.S. 2005. Critical science gaps impede use of no-take fisheries reserves. Trends in Ecology and Evolution 20:74-80.

Schumacher, J.D. and Kendall, A.W. Jr . 1991. Some interactions between young pollock and their environment in the western Gulf of Alaska. California Cooperative Oceanic Fisheries Investigations Reports 32:22-929.

Schumacher, J. D., Stabeno, P.J. and Bograd, S.J. 1993. Characteristics of an eddy over a continental shelf. Shelikof Strait, Alaska. Journal of Geophysical Research 98: 839 –8404.

Scheffer, M., Baveco, J.M., DeAngelis, D.L., Rose, K. A., Van Nes, E. H. 1995.Superindividuals: a simple solution for modelling large populations on an individual basis. Ecological Modelling 80: 161–170.

Shchepetkin, A.F. and McWilliams, J.C. 2005. The Regional Ocean Modeling System: A split-explicit, free-surface, topography-following coordinate ocean model. Ocean Modeling 9: 347-404.

Shields, G.F. and Gust, J.R. 1995. Lack of geographic structure in mitochondrial DNA sequences of Bering Sea walleye pollock, *Theragra chalcogramma*. Molecular Marine Biology Biotechnology 4: 69–82.

Smith, R.D. and Gent, P.R., 2002. Reference manual for the Parallel Ocean Program (POP): Ocean component of the Community Climate System Model (CCSM2.0 and 3.0). 74 pp. [HYPERLINK "http://www.cesm.ucar.edu/models/ccsm2.0.1/pop/doc/sci_ref_manual.pdf"http://www.cesm.ucar.edu/models/ccsm2.0.1/pop/doc/sci_ref_manual.pdf]

Stabeno, P.J. and Reed, R.K. 1994. Circulation in the Bering Sea basin by satellite tracked drifters. Journal of Physical Oceanography 24:848-854.

Stabeno, P.J., Reed, R.K. and Napp, J.M. 2002. Transport through Unimak Pass, Alaska. Deep-Sea Research II 49: 5919-5930.

Stabeno, P.J., Bond, N.A., Hermann, A.J., Kachel, N.B., Mordy, C.W. and Overland, J.E. 2004. HYPERLINK "http://www.pmel.noaa.gov/public/pmel/publications-search/search_abstract.php?fmContributionNum=2343"Meteorology and oceanography of the northern Gulf of Alaska. Continental Shelf Research 24 doi: 10.1016/j.csr.2004.02.007, 859–897.

Stockwell, J.D. and Johnson, B.M. 1997. Refinement and calibration of a bioenergetics-based foraging model for kokanee. Canadian Journal of Fisheries and Aquatic Science. 54: 2659-2676.

Stockwell, J.D. and Johnson, B.M. 1999. Field evaluation of a bioenergetics-based foraging model for kokanee (*Oncorhynchus nerka*). Canadian Journal of Fisheries and Aquatic Science 56(Suppl. 1): 140-151.

Sundby. S. 1983. A one-dimensional model for the vertical distribution of pelagic fish eggs in themixed layer. Deep Sea Research 30: 645-661.

Turnock, B.J., Wilderbuer, T.K., and Brown, E.S.. 2005. Gulf of Alaska arrowtooth flounder stock assessment. U.S. Department of Commerce, NMFS Stock Assessment and Fishery Evaluation Report. Anchorage, Alaska.

Werner, F.E., Mackenzie, B.R., Perry, R.I., Lough, R.G., Naimie, C.E., Blanton, B.O., and J.A. Quinlan, Larval trophodynamics, turbulence, and drift on Georges Bank: A sensitivity analysis of cod and haddock. Sciencia Marina 63 (Suppl. 1): 99-115, 2001.

Willis T.J., Millar R.B., Babcock R.C. and Tolimieri N. 2003. Burdens of evidence and the benefits of marine reserves: Putting Descartes before des horse? Environmental Conservation 30:97-103.

Wilson, M.T., Brodeur, R.D. and Hinckley, S., 1996. Distribution and abundance of age-0 walleye pollock, *Theragra chalcogramma*, in the western Gulf of Alaska during September 1990. in Brodeur RD, Livingston PA, Loughlin TR, Hollowed AB (eds) Ecology of Juvenile Walleye pollock , *Theragra chalcogramma*, U.S. Dept. Commerce., NOAA Tech. Rep. NMFS 126 p 11-24.

Wilson, M.T., Andrews, A.H. Brown A.L. and Cordes, E.E. 2002. Axial rod growth and age estimation of the sea pen, *Halipteris willemoesi* Kölliker. Hydrobiologia 471(1-3), 133–142

Yamashita, Y., and Bailey, K.M. 1989. A laboratory study of the bioenergetics of larval walleyepollock, *Theragra chalcogramma*. Fisheries Bulletin US 87: 525-536.

Yoklavich, M.M. and K.M. Bailey. 1990. Hatching period, growth and survival of young walleye pollock *Theragra chalcogramma* as determined from otolith abalysis. Marine Ecology Progress Series 64:13-23.

Figure captions

Figure 1. Map of the names of the areas used to set the spawning and nursery areas in eastern (EGOA), central (CGOA) and western the Gulf of Alaska (WGOA), the Aleutians (AL), the western (WBS) and eastern Bering Sea (EBS), the Arctic (AR) and the Basin (BAS) sectors. The spawning grounds corresponded (white circle) to the areas: 2: Inner Cook Inlet (InC), 3: Prince William Sound Inner (PWSin), 5: Outer Cook Inlet (OC), 6: Seward Inner (Sin), 8: Shelikof Strait North (SSN), 9: Kodiak Island North (KIN), 11: Shelikof Strait Exit (SSE), 12: Kodiak Island South (KIS), 14: Sutwik (Sut), 15: Semidi Islands (SemI), 17: Shumagin Islands Inner (SIin), 18: Shumagin Islands Outer (SIo), 20: Unimak Pass (UP), 21: Unimak Pass Outer (UPo). The potential nursery areas explored with the model were the same as the spawning areas (above) plus the following areas: 0: South East Alaska (SEA), 1: Yakutat (Yak), 4: Prince William Sound Outer (PWSo), 7: Seward Offshore (So), 10: Kodiak Island North Offshore (KINof), 13: Kodiak Island South Offshore (KISof), 16: Semidi Islands Offshore (SemIo), 19: Shumagin Islands Offshore (Siof), 22: Unimak Pass Offshore (UPof), 23: Unalaska Island (UI), 24: Unalaska Island offshore (UIof), 25: Chagulak Island (CI), 26: Adak (Ad), 27: Cobra Dane (CD), 28: Offshore (Off), 29: Bering Sea South Inner domain (BSSin), 30: Bering Sea South Middle domain (BSSm), 31: Bering Sea South Outer domain (BSSo), 32: Bering Sea South Basin (BSSb), 33: Bering Sea Central Inner domain (BSCin), 34: Bering Sea Central Middle domain (BSCm), 35: Bering Sea Central Outer domain (BSCo), 36: Bering Sea Central Basin (BSCb), 37: Bering Sea North Inner domain (BSNin), 38: Bering Sea North Middle domain (BSNm), 39: Bering Sea North Outer domain (BSNo), 40: Bering Sea North Basin (BSNb), 41: Arctic Inner domain (Arin), 42: Arctic Middle domain (Arm), 43: Arctic Outer domain (Aro), and 44: Arctic Basin (Arb)

Figure 2. Comparison of modeled Eulerian velocities (black) and observations from satellite-tracked Lagrangian drifters (red) deployed by the Alaska Fisheries Science Center (AFSC, NOAA) and the Pacific Marine Environmental Laboratory (PMEL).

Figure 3. Scatter plot between modeled and measured u (crosses) and v (circles) velocity component of the current.

Figure 4. The mean flow through Unimak Pass calculated at 40 m depth by month in the simulation years (dots). Positive values indicate flow through Unimak Pass to Bering Sea (Gulf of Alaska).

Figure 5. Contour map of modeled juvenile a) mean and b) coefficient of variation of densities on day of the year 215 showing potential nursery areas through the whole domain.

Figure 6. Retention of juvenile age-0 walleye pollock in each spawning area. a) Proportion of juvenile age-0 pollock retained in spawning areas where released, over all simulations. b) Proportion of juvenile age-0 pollock retained in spawning areas where released, by month of release (1st February, 1st March, 1st April, 1st May).

Figure 7. Proportion of age-0 juveniles that were alive at the end of the simulation (September 1st) by nursery area. The bars represent the month of release of the eggs.

Figure 8. Conceptual model of connectivity within the Gulf of Alaska (GOA) and between the GOA, the AL and BS based on potential spawning scenarios: Scenario A: only EGOA spawning

sector, Scenario B: only CGOA spawning sector, Scenario C: only WGOA spawning sector, and Scenario D: All spawning sectors combined.

Figure A1. Time-averaged modeled velocities (March through September) for the years a) 1978, b) 1982, c) 1988, d) 1992, e) 1999 and f) 2001. Speeds are shaded (m/s); normalized vectors indicate the direction.

Figure A2. Connectivity matrix showing proportion of age-0 juveniles that are found on September 1st in a specific nursery area for eggs released in a) February, b) March, c) April, and d) May.

Figure 1_B&W

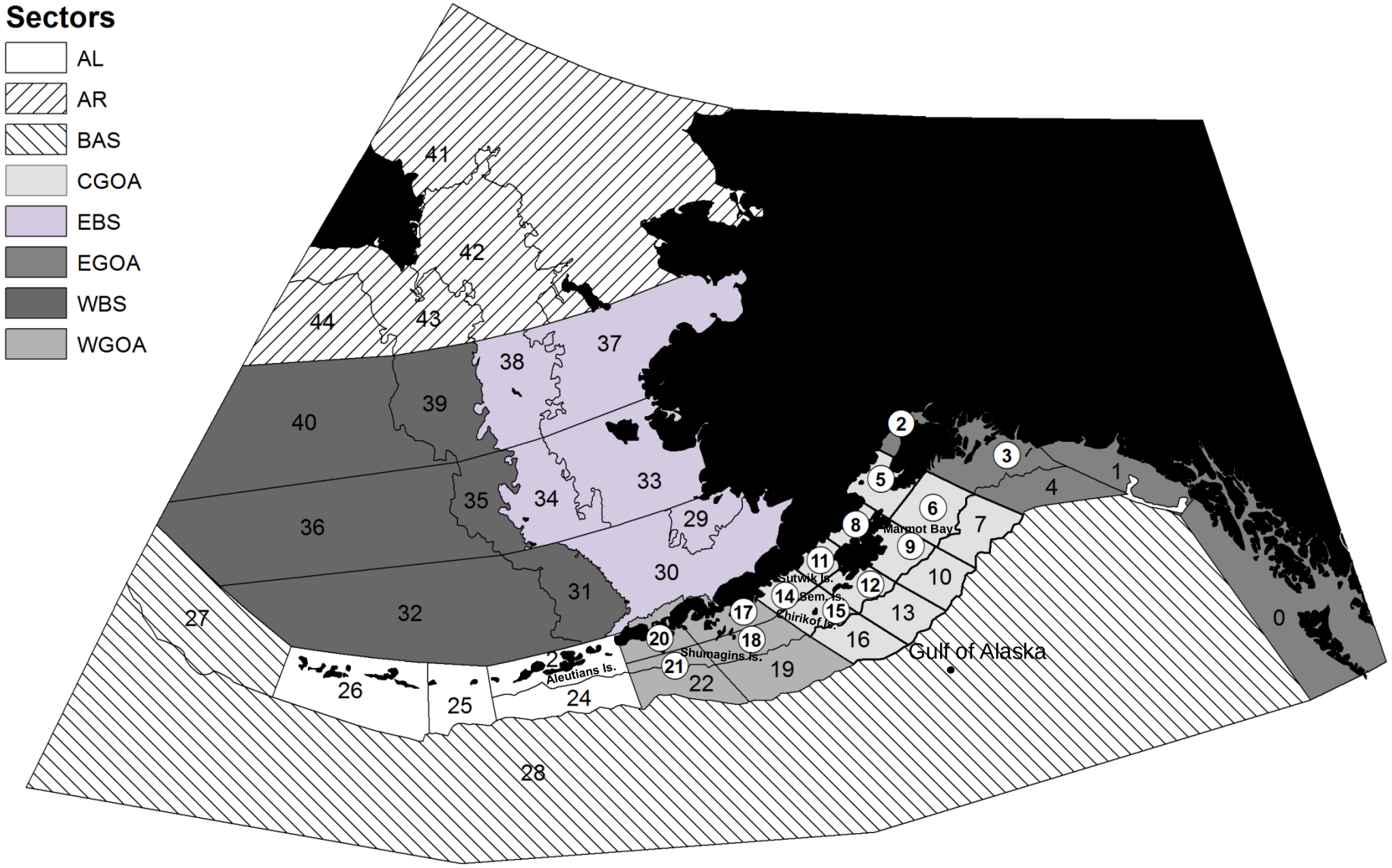
Sectors
AL
AR
BAS
CGOA
EBS
EGOA
WBS
WGOA
41
42
43
44
37
38
39
40
33
34
35
36
29
30
31
32
27
26
25
24
2
Aleutians Is.
28
22
19
20
21
Shumagins Is.
17
18
16
Gulf of Alaska
11
Sutwik Is.
14
Sem. Is.
15
Chirikof Is.
12
13
10
9
8
Marmot Bay
6
7
5
4
3
2
1
0

Figure 2_B&W

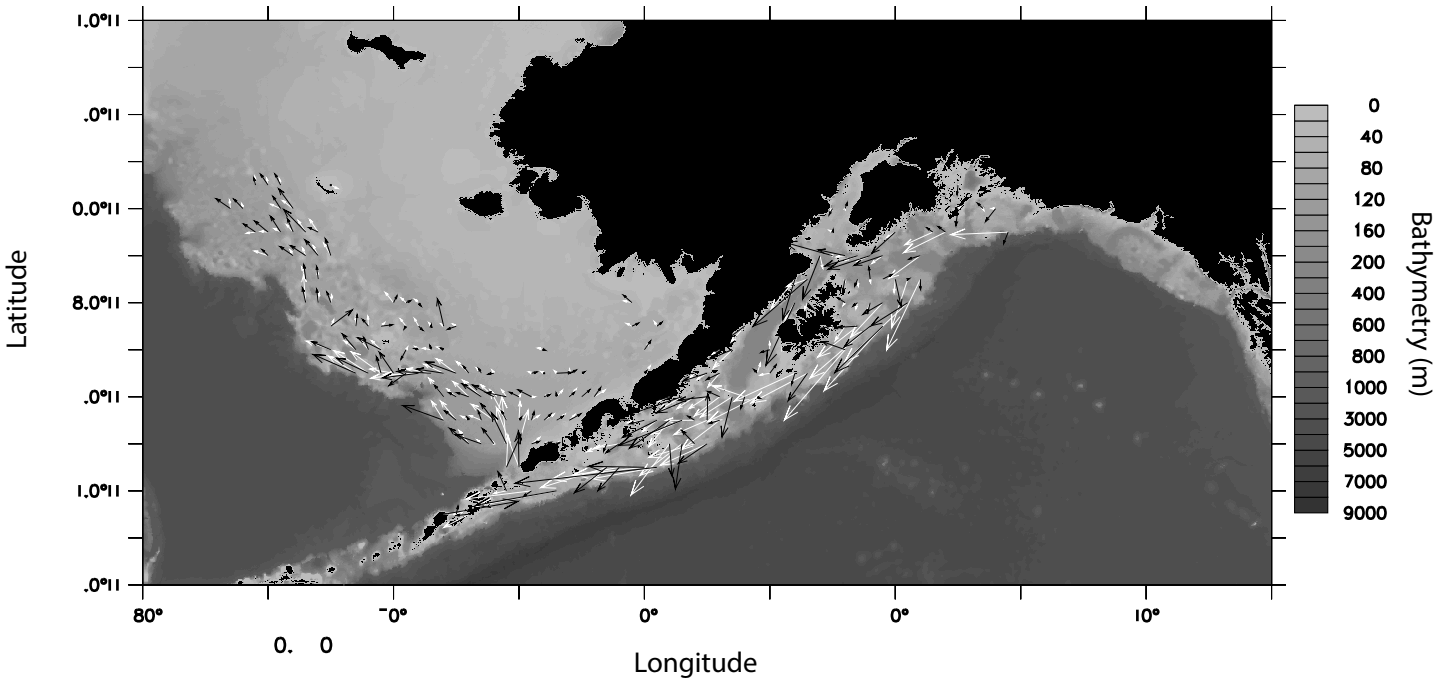
Latitude
Longitude
Bathymetry (m)
0
40
80
120
160
200
400
600
800
1000
3000
5000
7000
9000

Figure 2_color

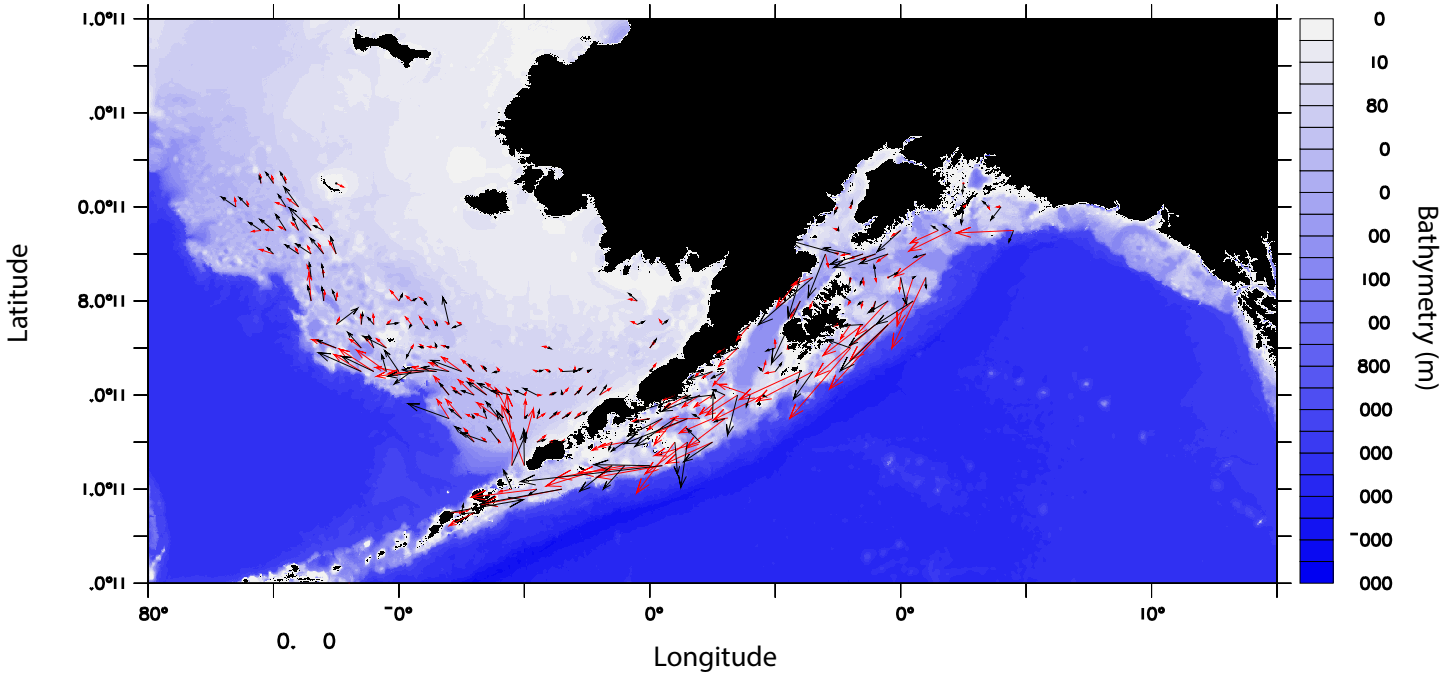

Figure 3_B&W

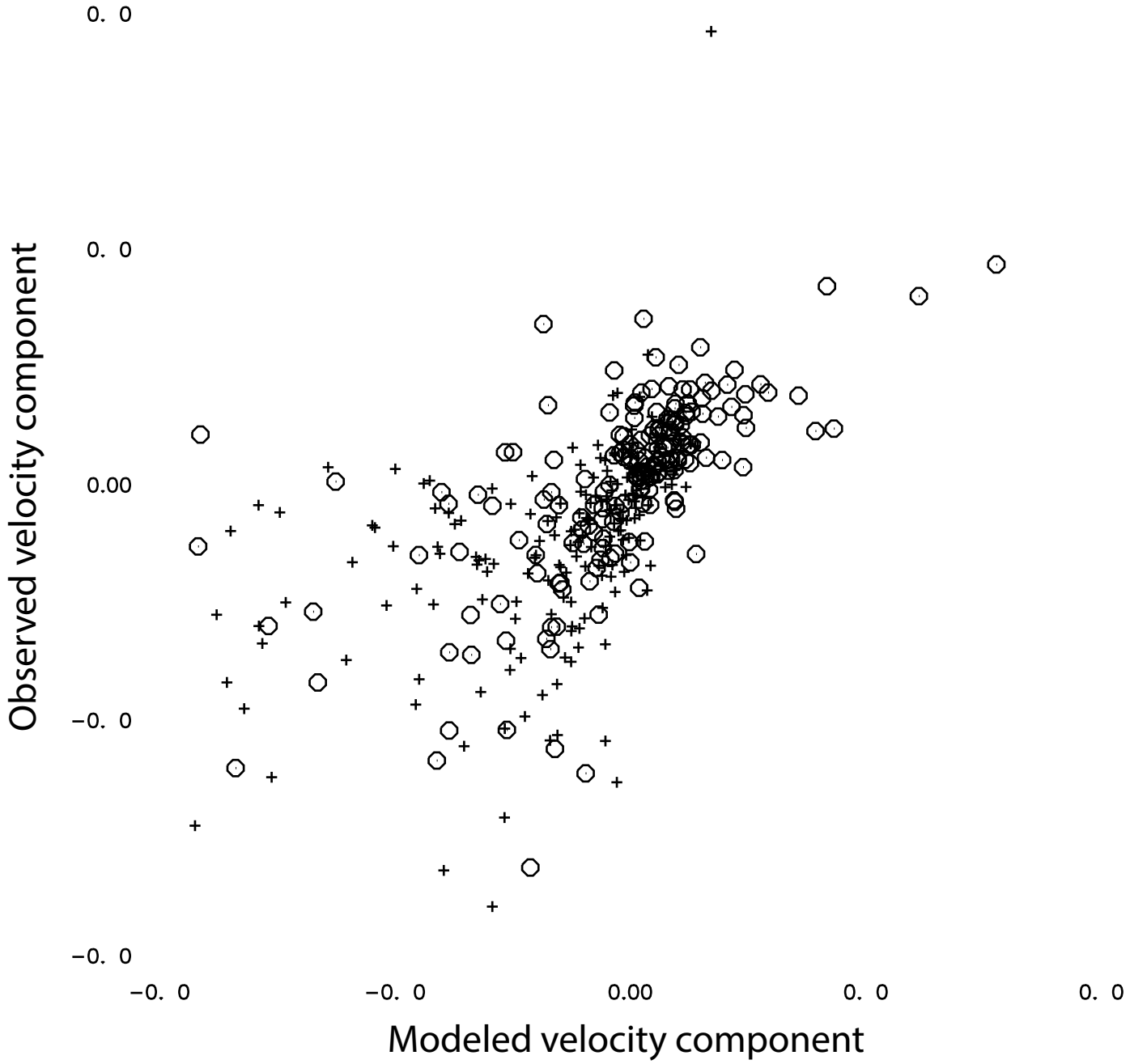
0. 0
0. 0
0.00
−0. 0
−0. 0
−0. 0
−0. 0
0.00
0. 0
0. 0
Observed velocity component
Modeled velocity component

Figure 4_B&W
Click here to download high resolution image

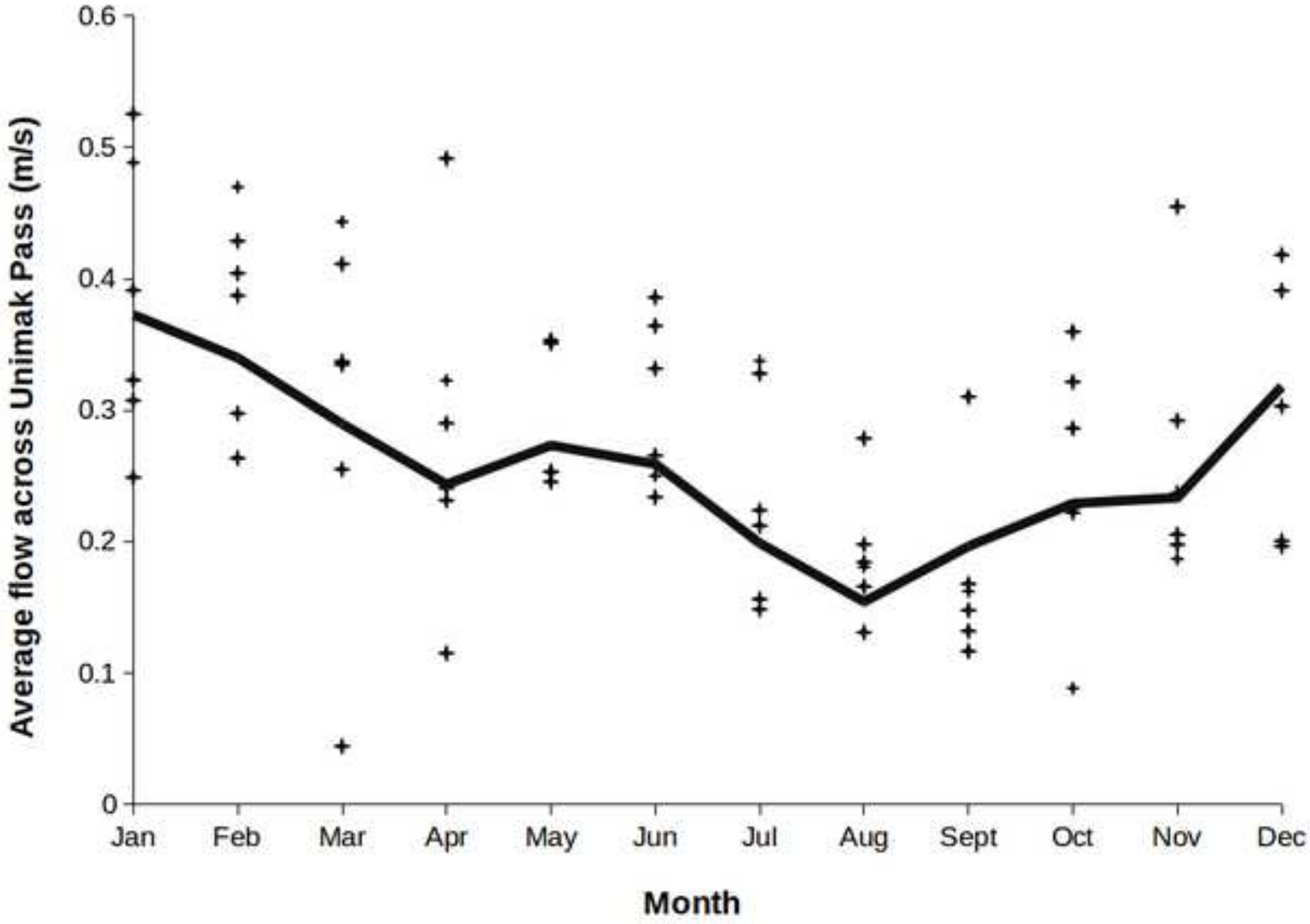

Figure 5 color

Click here to download high resolution image

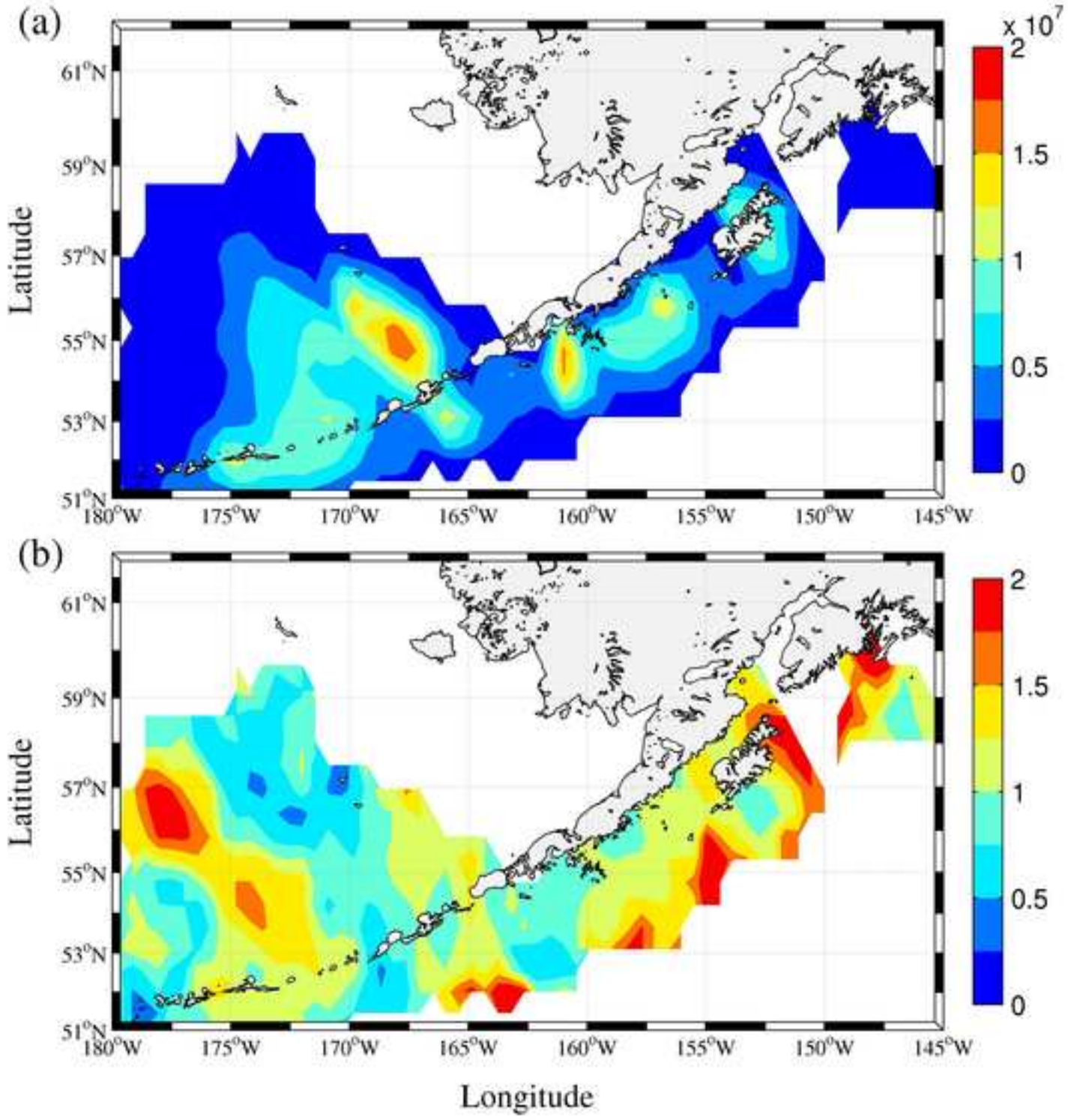

Figure 5 B&W

Click here to download high resolution image

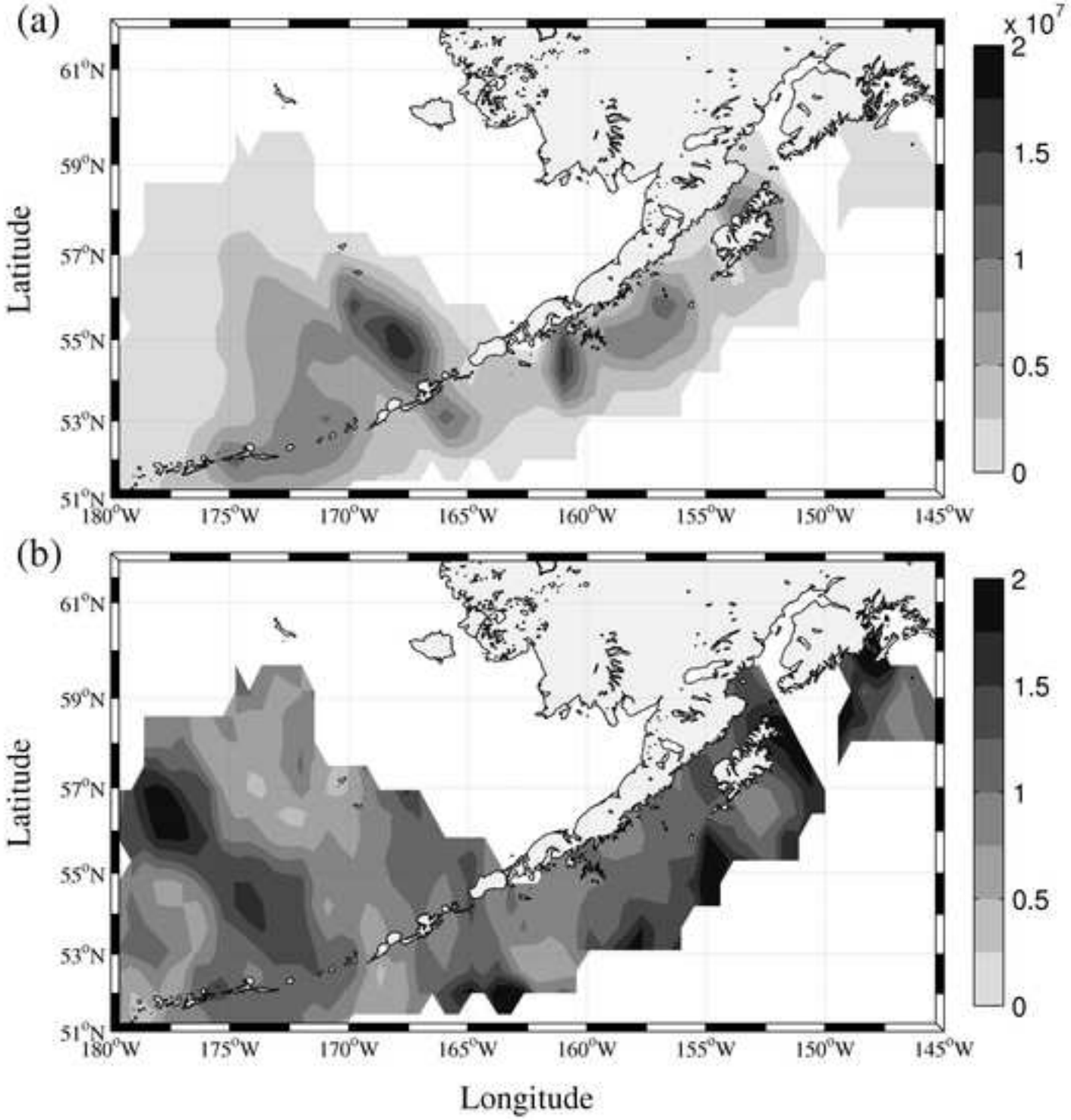

Figure 6 color

Click here to download high resolution image

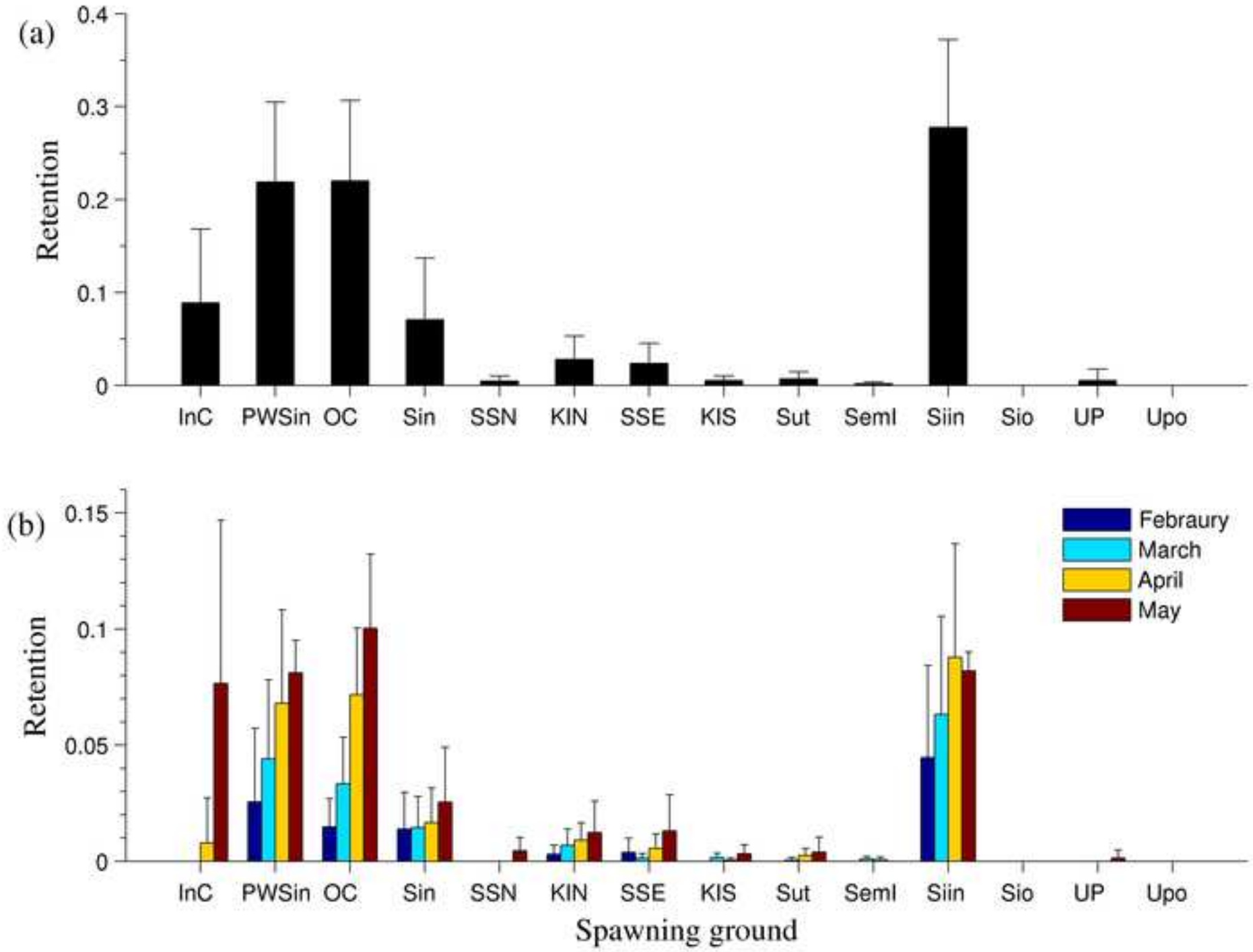

Figure 6 B&W

Click here to download high resolution image

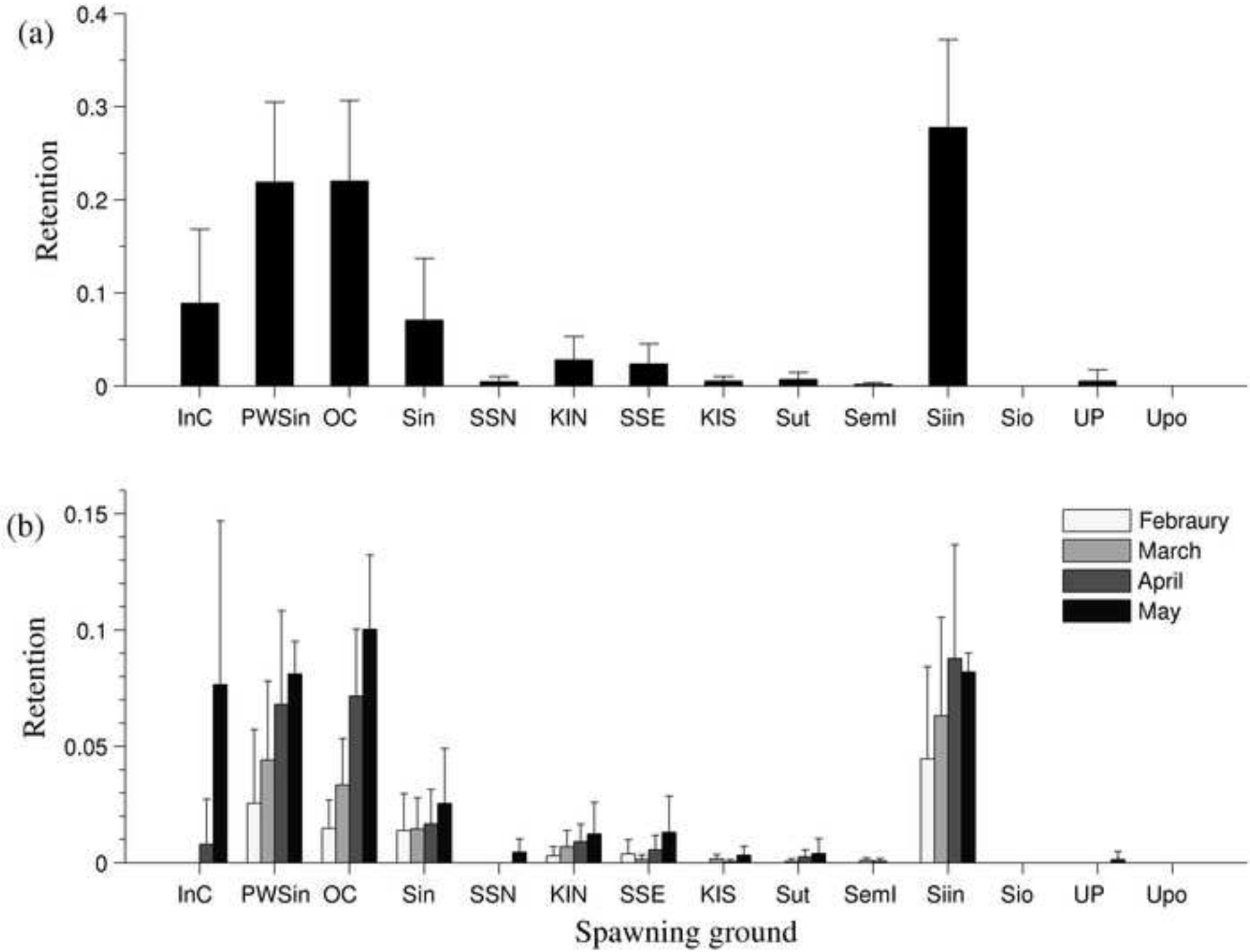

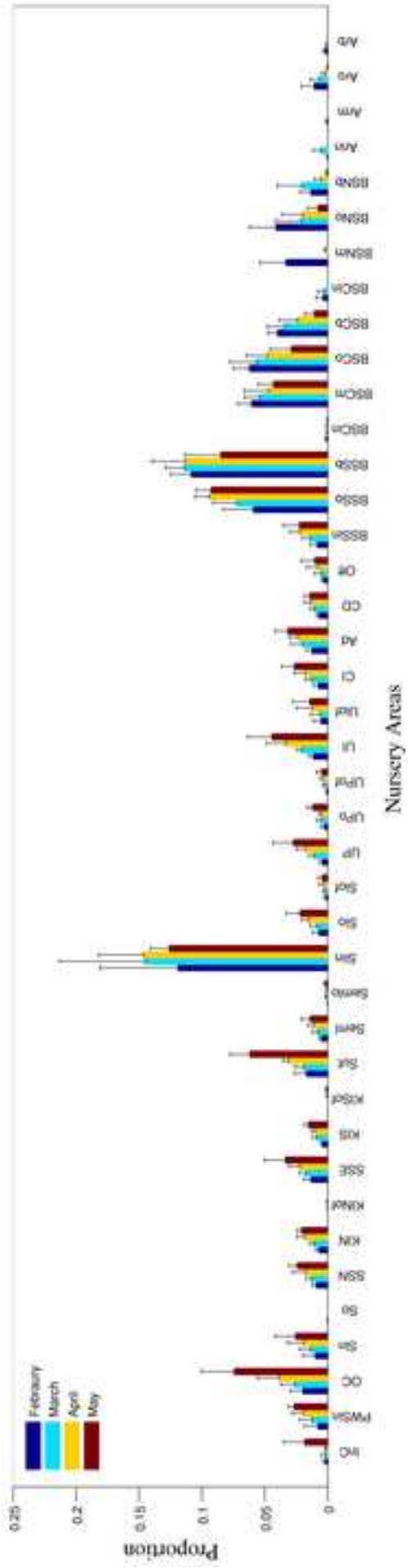

Figure 7 color
Click here to download high resolution image

Figure 7 B&W

Click here to download high resolution image

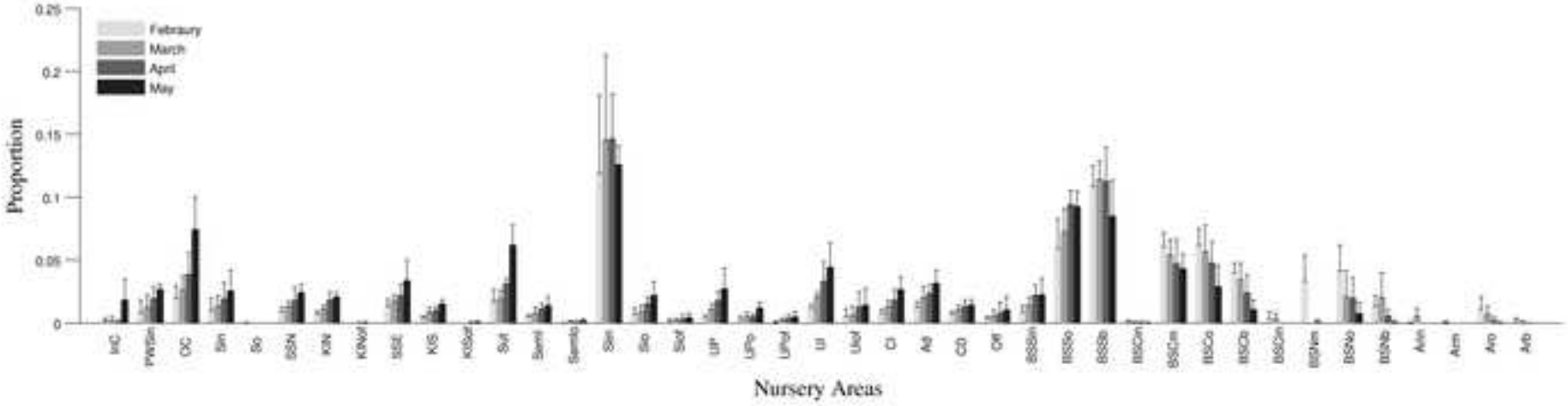

Figure 8_B&W

Click here to download high resolution image

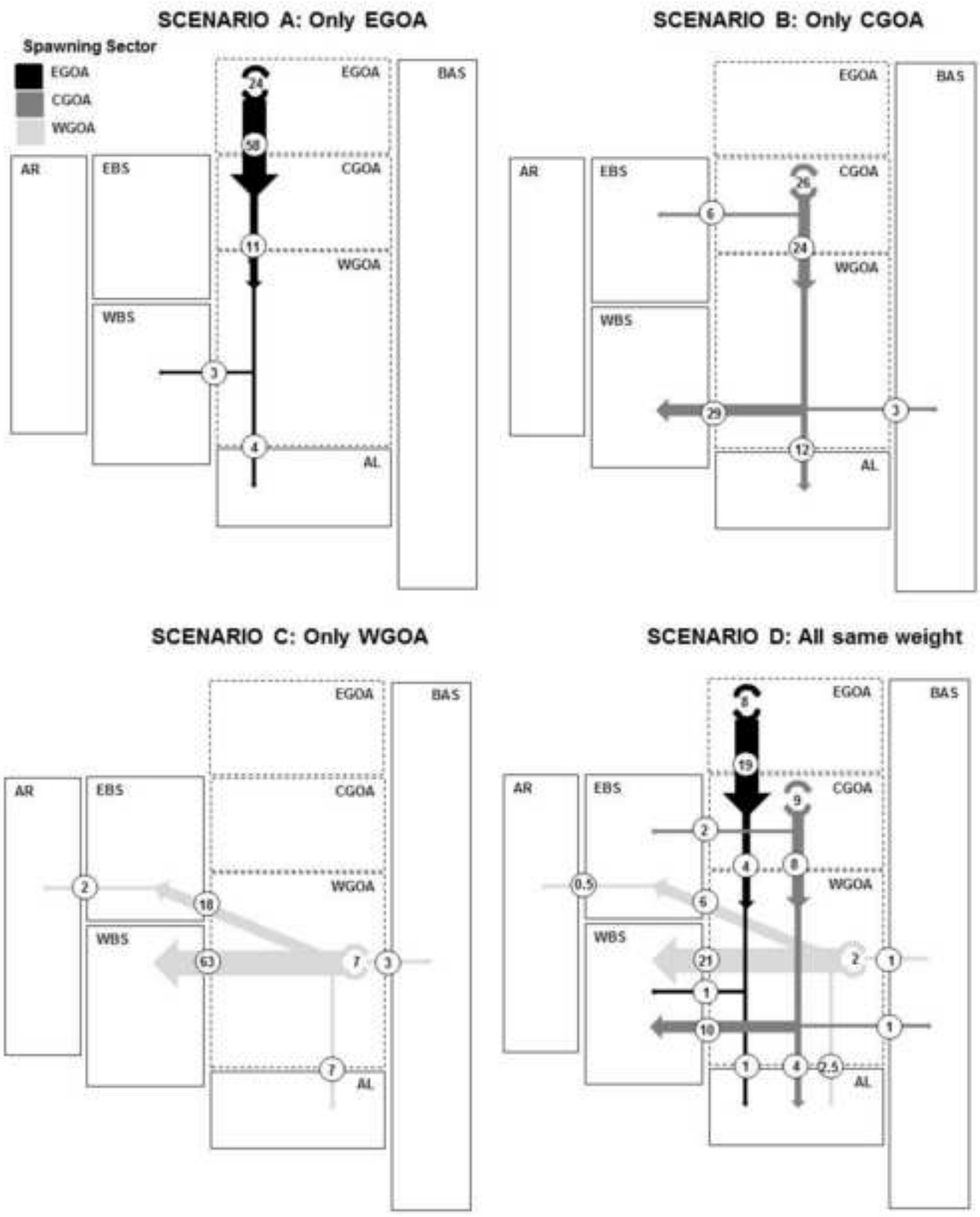

Table 1

Table 1. Known or suspected walleye pollock spawning and nursery areas in the Gulf of Alaska.

Areas	Observed area	Simulated area	References
Spawning ground	Shelikof Strait and Sea Valley	Shelikof Strait Exit (SSE), Shelikof Strait North (SSN), Semidi Islands (Seml), Sutwik Island (Sut)	[3]
	Shelf water to the Northeast of Kodiak island	Kodiak Iskand South (KIS), Kodiak Island North (KIN), Seward Inner (Sin), Outer Cook Inlet (OC)	[3]
	Vicinity of Shumagin Islands to the Southwest	Shumagin Islands Inner (SIin) and outer (Sio), Unimak Pass (UP) and outer (Upo)	[3]
	Inner Cook Inlet	Inner Cook Inlet (InC)	[4]
	Entrance to Prince William Sound	Prince Williams Sound Inner (PWSin)	[1,2]
	Middleton Island	Seward Inner (Sin)	[1,2]
	Marmot Bay	Kodiak Island North (KIN)	[1,2]
	Shelikof Strait	Shelikof Strait North (SSN) Shelikof Strait Exit (SSE)	[1,2]
	Chirikov shelf break	Semidi Islands (Seml)	[1,2]
	Shumagin Gully	Shumagin Islands Inner (SIin)	[1,2]
	Morzhovoi Bay	Unimak Pass (UP)	[1,2]
Nursery ground	Shumagin area from Semidis islands to Unimak Pass	Sutwik Island (Sut)	[5,6,7]
		Semidi Islands (SemI)	[5,6,7]
		Shumagin Islands Inner (SIin)	[5,6,7]
		Shumagin Islands Outer (SIo)	[5,6,7]
		Unimak Pass (UP)	[5,6,7]
		Unimak Pass Outer (UPo)	[5,6,7]
	North of Kodiak Island	Outer Cook Inlet (OC)	[5,6,7]

		[5,6,7]
	Seward Inner (Sin)	
North East of Kodiak Island	Kodiak Island North (KIN)	[5,6,7]
Southwest of Unimak Pass	Unimak Pass (UP)	[5,6,7]

[1] The areas have been identified by Ecosystems and Fisheries-Oceanography Coordinated Investigations (ECO Foci) cruises as spawning regions. [2] The Shelikof Strait Acoustic Survey estimates by NFMS (Dorn *et al*., 2013). [3] Doyle *et al*., (this issue).[4] Rodrigues *et al*. (2006).[5] Brodeur and Wilson, 1996. [6] Wilson *et al.*, 1996. [57] Wilson, 2000.